Planetary and Space Science 180 (2020) 104766

Contents lists available at ScienceDirect

Planetary and Space Science

journal homepage: www.elsevier.com/locate/pss

On the impact of the operational and technical characteristics of the LaRa experiment on the determination of Mars' nutation

S. Le Maistre [a,*], M.-J. Péters [a], J.-C. Marty [c], V. Dehant [a,b]

[a] Royal Observatory of Belgium, Brussels, Belgium
[b] Université catholique de Louvain, Louvain-la-Neuve, Belgium
[c] Centre National d'Etudes Spatiales, Toulouse, France

ABSTRACT

LaRa is a radio-science payload of the ExoMars 2020 mission. The LaRa instrument consists of an X-band transponder accompanied by a set of three antennas and three RF cables, all mounted on the stationary ExoMars surface platform. This instrument is designed to measure with a couple of mHz of accuracy the Doppler shift induced by the variations in Mars rotation and orientation on a direct-to-Earth round-trip radio link. The main scientific objective of the LaRa experiment is to constrain the interior structure of Mars by precisely measuring the nutations of the planet's spin axis. LaRa's measurements will also be used to refine the rotation model of Mars and infer constraints on the dynamic of its atmosphere. This paper aims at characterising the impact of different parameters, related to the design of the LaRa instrument itself and to its operations, on the determination of the rotation and orientation parameters of Mars, and especially on the nutation parameters. Among other quantities, we analyze the effects of the measurements noise, the tracking pass length and occurrence, the mission duration, the radio signal elevation and azimuth in the lander sky, the blackout periods, and the onboard power availability. The work is a comparative study, where we examine different scenarios/cases with respect to a nominal one. From this study, general conclusions can be drawn on the nutation determination from direct-to-Earth Doppler data provided by a landed mission (like InSight). This study provides quantitative inputs that can be used for the programmatic and operation strategy of a radio-science experiment from a lander. In particular, we show that regular tracking from both East and West sides of the lander (i.e. at Earth-rises and Earth-sets) is mandatory to best fit the rotation parameters. Since power issues are frequent on solar-powered landers, we might have to wait for the spacecraft batteries to recharge before operating LaRa. This study shows that turning on LaRa up to one hour after sunrise (i.e. $\leq 15^{\circ}$ of Sun elevation) is acceptable, while requiring higher elevation of the Sun to operate LaRa would significantly reduce its science return. One can finally mention that blackout periods of any kind would compromise the scientific achievement of the LaRa experiment if last too long (hundreds of days).

1. Introduction

LaRa is a scientific payload of the ExoMars 2020 mission to be launched by the European Space Agency (ESA) and the Russian space agency (Roscosmos) in July 2020. This mission uses a Russian carrier module to deliver a European rover on the surface of Mars. The carrier module will remain steady and operational on Mars surface for at least one Earth year. This Surface Platform (SP) will carry 13 scientific instruments including LaRa.The LaRa instrument consists of an X-band coherent transponder, a receiving antenna and two transmitting antennas for which the flight model has just been delivered for integration on the Russian surface platform (Dehant et al., 2019). The LaRa experiment main objective is to refine the rotation model of Mars in order to better constrain the planet's interior structure and atmosphere dynamics. In particular, LaRa will improve the current determination of the precession rate of the planet and measure its nutation precisely enough to quantify the effect of the liquid core. Likewise the tidal Love number, nutations will then provide an independent means to confirm the presence of the liquid core and allow for inferences about its structure.In this paper, we present the results of simulations that address the impact of several operational parameters on the determination of the Mars Orientation and rotation Parameters (MOP). All the numerical simulations have been performed using the GINS (Geodésie par Intégrations Numériques Simultanées) software. It has been developed by Centre National d'Etudes Spatiales (CNES) and further adapted at the Royal Observatory of Belgium to allow for planetary applications involving surface landers. We provide first a nominal case, considered as a reference for all the other cases and for which all the parameter estimates are given (see Sec. 2). The other sections of this document will present and comment only the nutation parameters framed in red in Fig. 4, namely the semi-annual prograde nutation amplitude (p_2) and the ter-annual retrograde nutation amplitude (r_3). These amplitudes are considered to be of prime importance in the detection of the liquid core contribution in the nutation signal (e.g. Le Maistre et al. (2012)). Indeed, as shown in Fig. 1, p_2 (+1/2

* Corresponding author.
E-mail address: sebastien.lemaistre@oma.be (S. Le Maistre).

https://doi.org/10.1016/j.pss.2019.104766
Received 24 July 2019; Received in revised form 2 October 2019; Accepted 4 October 2019
Available online 14 October 2019

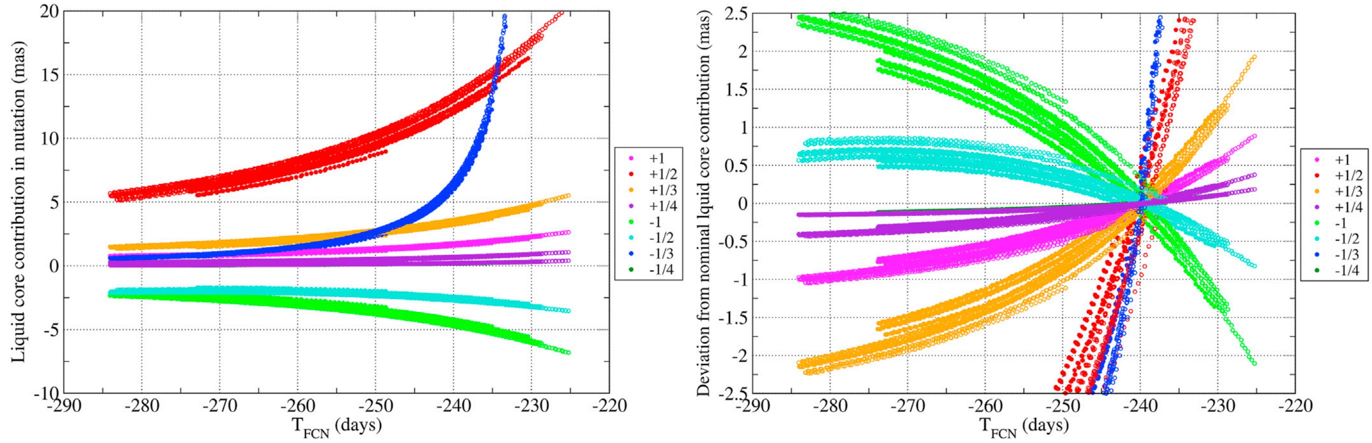

Fig. 1. Left panel: Liquid core contribution in the amplitudes of nutation in prograde/retrograde terms as function of the Free Core Nutation (FCN) period in days. Colors are the amplitudes of different periods of rigid nutation (update of Fig. 10.a of Le Maistre et al. (2012)). Right panel: Variations as a function of T_{FCN} of the liquid core contribution in the prograde/retrograde amplitudes of nutation relatively to the nominal amplitudes at $T_{FCN} = -240$ days. (For interpretation of the references to color in this figure legend, the reader is referred to the Web version of this article).

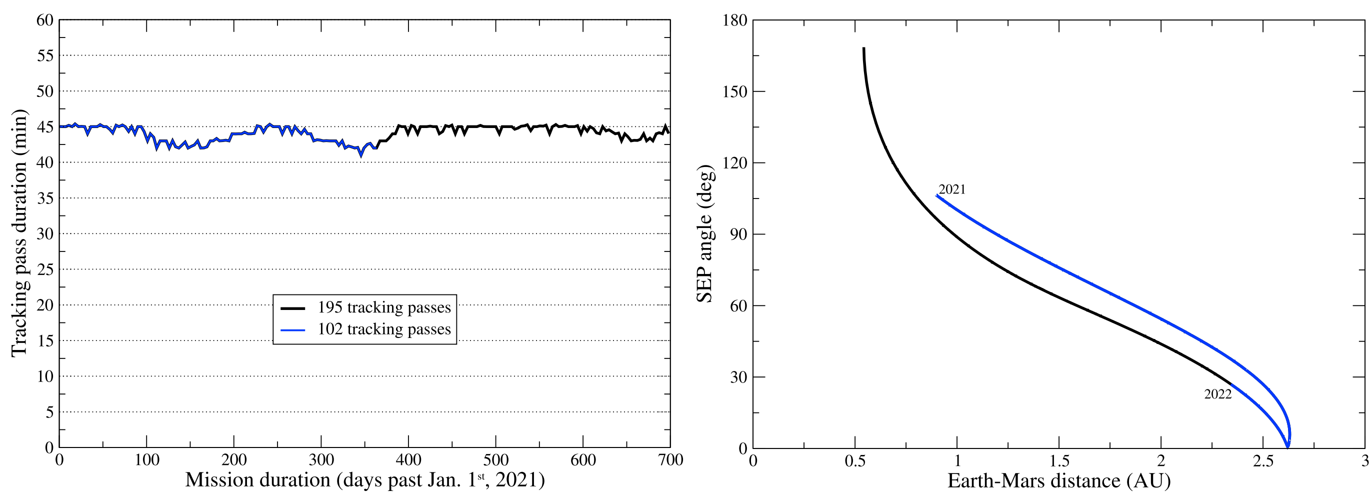

Fig. 2. Nominal tracking pass length (left panel) and Earth-Mars configuration in term of distance and Sun-Earth-Probe (SEP) angle (right panel). The blue part of the curve corresponds to the first Earth year after the Mars landing (nominal mission) while the black part corresponds to the second Earth year of mission (extended mission). (For interpretation of the references to color in this figure legend, the reader is referred to the Web version of this article).

red curve) and r_3 (-1/3 blue curve) are expected to be significantly amplified by the presence of a liquid core. The amplitudes of the other sub-harmonics are expected to vary only by up to ± 2.5 milliarcsecond (mas) with respect to their reference value obtained by assuming that the Free Core Nutation (FCN) period equals -240 days (Folkner et al., 1997, 2018) (Fig. 1 right panel). This is quite small with respect to p_2 and r_3 variations as a function of the FCN period.

2. The nominal scenario

2.1. Simulation setup

The simulations carried out and discussed in the present paper are deviations from a nominal scenario, which corresponds to the LaRa experiment as proposed and selected to fly onboard the Russian surface platform of the ExoMars 2020 mission (Dehant et al., 2009, 2011, 2019). The nominal case is depicted by the following characteristics:

- Landing site at Oxia Planum (335.45° E, 18.20° N, -2.5 km),
- 45 min of tracking per session as shown on Fig. 2 left panel (note that 15 min of acquisition time has been removed from the one-hour baseline mentioned in Dehant et al. (2019)),
- Tracking sessions twice a week (every 3.25 days and not 3.5 days in order to have the wanted azimuthal distribution as explained below),
- Doppler data affected by a white noise of 0.05 mm/s at 60s of integration time,
- Doppler data acquired within the range of [35;45]° of elevation above the local horizon of the surface platform (see Fig. 3),
- Doppler tracking with a Line-Of-Sight to the Earth alternatively coming from the East and from the West azimuth direction (switch every tracking session, see Fig. 3),
- 700 days of operation, starting from January 1st, 2021. The ExoMars platform nominal mission is only one Earth year, but the LaRa transponder is designed to work at least one Martian years (687 days), that is why we choose 700 days as a baseline.
- Three Deep-Space-Network (DSN) ground stations to track LaRa. They are placed approximately 120° apart, one at Goldstone, in California's Mojave Desert; one near Madrid, Spain; and one near Canberra, Australia.

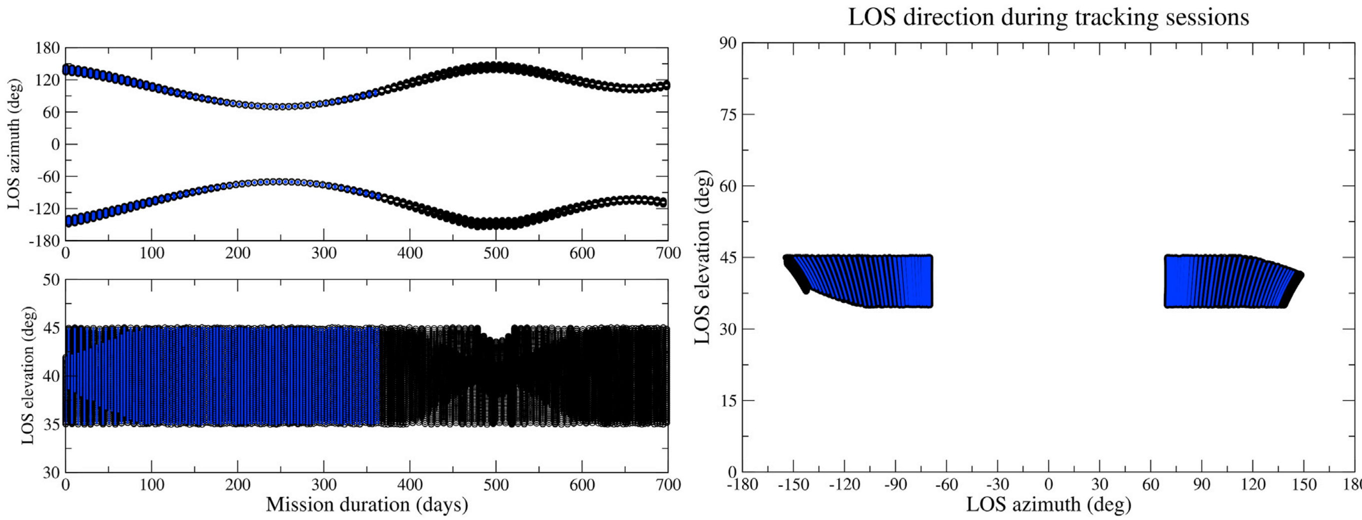

Fig. 3. Earth Line-Of-Sight (LOS) azimuth and elevation during the nominal tracking sessions. The blue part of the curve corresponds to the first Earth year after the Mars landing (nominal mission) while the black part corresponds to the second Earth year of mission (extended mission). (For interpretation of the references to color in this figure legend, the reader is referred to the Web version of this article).

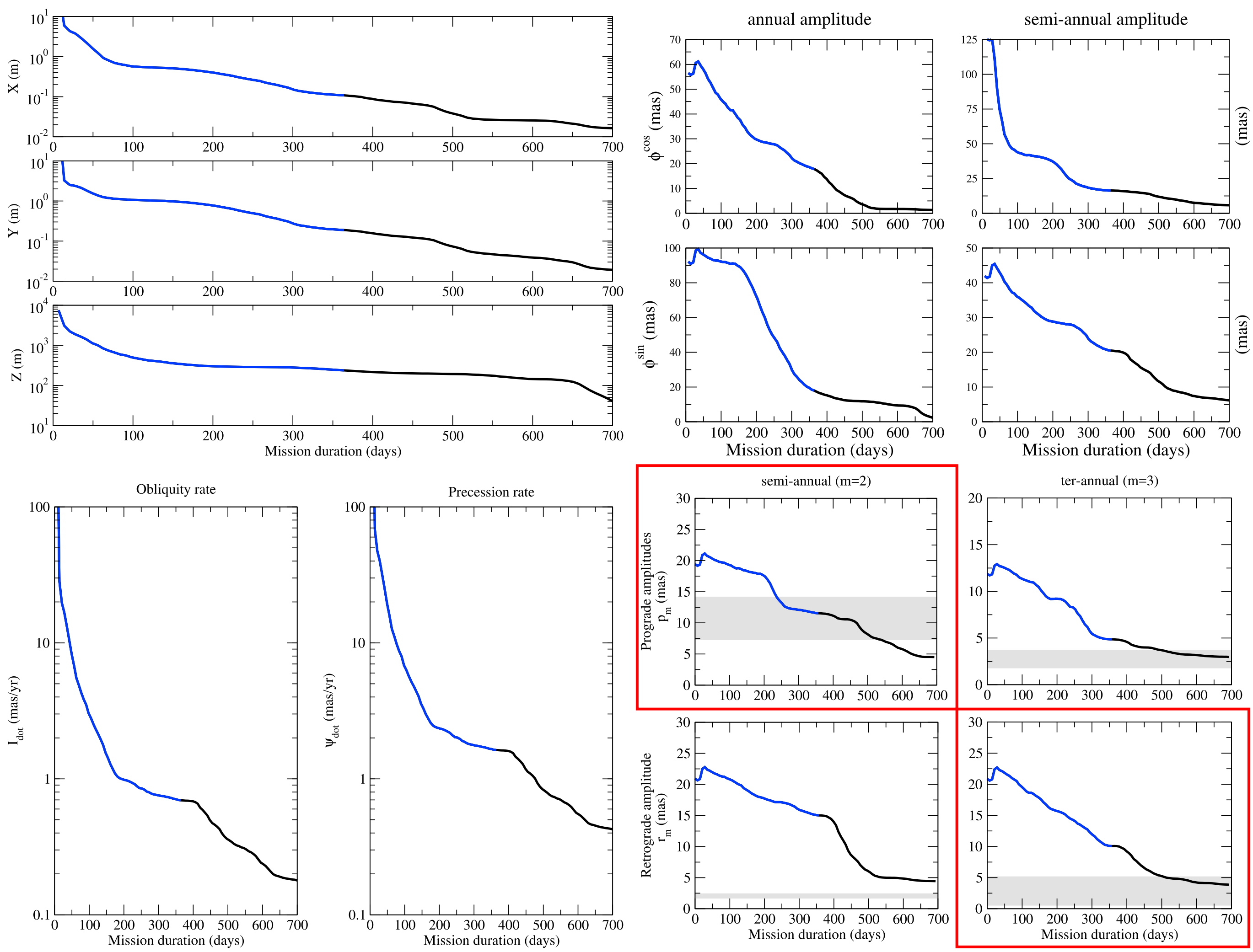

Fig. 4. Uncertainties of the estimated MOP and lander coordinates in the nominal scenario. In red frames are the nutation parameters that will serve as reference for all the simulations of the following sections. The one-Earth-year nominal mission of ExoMars (2020) surface platform is highlighted in blue on each graph. (For interpretation of the references to color in this figure legend, the reader is referred to the Web version of this article).

2.2. The rotation model

The synthetic Doppler data are built following the description given above (see Figs. 2 and 3) and according to the rotation model reported in Table 1. This "truth model" is in very good agreement with the recently published models of Kuchynka et al. (2014) and Konopliv et al. (2016). The prograde and retrograde amplitudes reported in Table 1 are those of a hypothetical flattened rigid planet. They are computed from the amplitudes in obliquity and longitude given by Roosbeek (1999). To create the Doppler data, the latter are augmented with a model for the non-rigid planet with a fluid core as used for the analysis of the historical data (Viking, Pathfinder and MER's data) by Kuchynka et al. (2014) and Konopliv et al. (2016). The synthetic Doppler data are also created accounting for the polar motion as proposed by Van den Acker et al. (2002). It was not considered useful to put the latter in Table 1. Details on the rotation model of Mars can be found in Konopliv et al. (2006); Le Maistre et al. (2012, 2018); Le Maistre (2013).

2.3. Set of estimated parameters

Among all the MOP of Table 1, which have been used to create the simulated Doppler data, we only estimate a subset of parameters. Typically, all the simulations performed hereafter are simultaneously estimating the lander position cartesian coordinates (x, y, z), the planet precession rate $(\dot{\psi}_0)$ and obliquity rate $(\dot{I}_0)$, the spin angle variations amplitudes (annual and semi-annual) and the nutation amplitudes (semi-annual and ter-annual). Following Le Maistre et al. (2012), the other MOPs are maintained fixed because they can be considered as well-known given the accuracy of LaRa's measurements (i.e. with a signature in the Doppler, which is well below noise level). This strategy of estimation will be refined in a near future and such settings might then change. However, such changes in the parameters set and in the adjustment strategy should not modify the predictions and conclusions of the following simulations.

The estimated parameters are a priori perturbed by 100% of the liquid contribution for the nutation and by up to 20% of their own value for the others (comparable to settings in Le Maistre et al. (2012, 2018)). It is worthwhile to mention that the actual values of the a priori errors (difference between the values of the truth model parameters and the a priori values attributed to each estimated parameters) are of little importance here because:

- The Doppler observables depend linearly on the MOP parameters considered herein,[1] which yields to a posteriori uncertainties (mostly) independent from the actual value of the parameters themselves,
- We are mainly interested by the formal errors (also called here after uncertainties or precisions), and consider the true errors (differences between the values of the truth model parameters and those of the estimated parameters) only when relevant.

A priori constraints on spin angle parameter (also called ΔLOD hereafter) are set to 20% of the truth model. The a priori constraints in nutation amplitudes are set to 200% of the largest possible contribution of a liquid core, which is computed (from Eqs. (2) and (3) below) assuming $T_{FCN} = -230$ days and $F = 0.12$.

The present paper focuses on the nutation parameters, which are prime objectives of the LaRa experiment because they will provide important constraints on the interior structure of Mars (e.g. Dehant et al. (2000, 2019); Van Hoolst (2007, 2015); Le Maistre et al. (2012)). The nutation parameters studied are p_m and r_m, the amplitudes of the complex prograde and retrograde nutation terms. They are related to the classical nutation amplitudes (Defraigne et al., 1995) in obliquity $(I_m^{c,s})$ and longitude $(\psi_m^{c,s})$ by:

$$p_m e^{\frac{2i\pi}{T_m}t} + r_m e^{-\frac{2i\pi}{T_m}t} = I_m^c \cos\left(\frac{2\pi}{T_m}t\right) + I_m^s \sin\left(\frac{2\pi}{T_m}t\right) + i \sin I_0 \left(\psi_m^c \cos\left(\frac{2\pi}{T_m}t\right) + \psi_m^s \sin\left(\frac{2\pi}{T_m}t\right)\right), \quad (1)$$

where $i^2 = -1$ and I_0 is the mean obliquity of Mars at J2000. The forcing periods are the harmonics of Mars orbital periods. T_1 (i.e. $m = 1$) is the annual period of 687 terrestrial days and the next harmonic periods $(m \geq 2)$ correspond to the semi-annual (343.5d), the ter-annual (229d), the quarter-annual (171.7d), etc. As shown in Table 1, the truth model includes the first six periods of nutation, but, as said before, we only estimate p_2, p_3, r_2 and r_3 for the nutation.

Table 1
Mars rotation model used as the truth model to create the synthetic Doppler data, along with the a priori constraints on the estimated MOP. Angles at epoch (I_0, ψ_0, φ_0), rates $(\dot{I}_0, \dot{\psi}_0, \dot{\varphi}_0)$ and spin angle amplitudes are from Konopliv et al. (2016). The amplitudes of the truth model of nutation are computed from the model of rigid nutation of Roosbeek (1999) modulated by a liquid core of FCN period and core factor reported at the end of the table. The nutation amplitudes are given for the rigid case and for the fluid core case (rigid/fluid).

Parameter	Symbol	Truth model
Obliquity at t_0 (deg)	I_0	25.189
Longitude at t_0 (deg)	ψ_0	81.97
Prime meridian at t_0 (deg)	φ_0	133.386
Obliquity rate (mas/year)	$\dot{I}_0$	−2.0
Precession rate (mas/year)	$\dot{\psi}_0$	−7608.3
Rotation rate (deg/day)	$\dot{\varphi}_0$	350.891985307
1-annual cosine spin angle (mas)	φ_1^c	481
1/2-annual cosine spin angle (mas)	φ_2^c	−103
1/3-annual cosine spin angle (mas)	φ_3^c	−24
1/4-annual cosine spin angle (mas)	φ_4^c	−6
1-annual sine spin angle (mas)	φ_1^s	−155
1/2-annual sine spin angle (mas)	φ_2^s	−93
1/3-annual sine spin angle (mas)	φ_3^s	5
1/4-annual sine spin angle (mas)	φ_4^s	8
1-annual prograde nutation (mas)	p_1	102/104
1/2-annual prograde nutation (mas)	p_2	498/512
1/3-annual prograde nutation (mas)	p_3	108/112
1/4-annual prograde nutation (mas)	p_4	18/18
1/5-annual prograde nutation (mas)	p_5	3/3
1/6-annual prograde nutation (mas)	p_6	0.5/0.5
1-annual retrograde nutation (mas)	r_1	137/132
1/2-annual retrograde nutation (mas)	r_2	18/15
1/3-annual retrograde nutation (mas)	r_3	5/12
1/4-annual retrograde nutation (mas)	r_4	1/1
1/5-annual retrograde nutation (mas)	r_5	0/0
1/6-annual retrograde nutation (mas)	r_6	0/0
Core momentum factor	F	0.07
FCN period (days)	T_{FCN}	−240

2.4. MOP estimates in nominal case

In this section, we discuss the parameters that are all systematically estimated for each scenario considered in the sections below. However, in the next sections, we only present results about the nutation parameters framed in red in Fig. 4.

Fig. 4 shows the uncertainties of all the estimated parameters as a function of the mission duration. They correspond to one time the formal errors provided by the least square method used in GINS. We assume that these uncertainties are relevant quantities (i.e. close to realistic errors) since the real LaRa data will be whitened before analysis[2] and because

[1] Except for T_{FCN} which is mentioned in this section but no longer discussed in the rest of the paper.

[2] As most orbit determination software, the GINS uses a least squares filter approach where tracking measurements are assumed to be uncorrelated, i.e. white noise contaminated. If the noise is not white then the observations should be whitened prior to filtering in order to obtain the unbiased minimum variance estimate of the parameters (see Mackenzie and Folkner (2006)).

there are usually no significant systematic errors on modern radio-science experiments onboard a lander.The upper left panel in Fig. 4 shows the time evolution of the estimated uncertainties on the lander coordinates. It can be seen from the figure that LaRa will be able to rapidly determine the Russian platform location at the surface of Mars with a precision of few centimetres in the equatorial components X and Y, but the precision along the spin axis, Z, will only be determine with a precision of tens of meters, even after 700 days of operation. Note that Le Maistre (2016) has proposed a simple method to reduce the uncertainties of Z to a few meters in few days just by using a high-resolution topography model of the landing site area (but with no additional data). For further details, the reader should consult Dehant et al. (2019).

On Fig. 4 top right panel, we see that LaRa will reduce the ΔLOD uncertainties by a factor up to 10 with respect to the precision of the last rotation model published by Konopliv et al. (2016).[3]

The precession rate of Mars will be determined by LaRa with an uncertainty of ~0.4 mas/year after one Martian year (see Fig. 4 bottom left panels). This is 5 times better than the precision of Konopliv et al. (2016) best solution. The impact of such an improvement on the determination of the planet polar moment of inertia and consequently on the interior structure of Mars is discussed in Dehant et al. (2019).The estimated uncertainties on the amplitudes of the semi- and ter-annual pro- and retro-grade nutation as a function of the mission duration are shown on the bottom right panels of Fig. 4. The four parameters uncertainties are superimposed with the expected effect a planet with a liquid core would have on those nutations (grey boxes in the graph framed in red). When the parameters uncertainties are smaller than the liquid core contributions to nutation, represented by these grey shaded boxes, then data accumulated by LaRa allow to detect the effect of the liquid core on the signal. As we can see on the graph, this should be the case after at least 250 days of mission on the semi-annual prograde amplitude and after at least 500 days of mission on the ter-annual retrograde amplitude (focusing on the target parameters, p_2 and r_3). The surface of the grey shaded boxes are calculated from current knowledge about interior structure parameters of Mars (within their 1σ error bars), assuming the core in hydrostatic equilibrium. This knowledge constrains the FCN period to a range of [-241.9; -284] days, and the core momentum factor F to 0.02 and 0.057. This is significantly away from the resonance values (when T_{FCN} is very close to the ter-annual period of -229d and F is about 0.12, see Le Maistre et al. (2012)) and from the nominal values of T_{FCN} = -240d and $F = 0.07$ (e.g. Folkner et al. (1997)). From the ranges of T_{FCN} and F, the amplification factors of the rigid prograde and retrograde amplitudes can be computed according to

$$\frac{p'_m}{p_m} = 1 + F\frac{T_{FCN}}{T_{FCN} - T_m}, \tag{2}$$

$$\frac{r'_m}{r_m} = 1 + F\frac{T_{FCN}}{T_{FCN} + T_m}, \tag{3}$$

where the primed quantities are the amplitudes of nutation for a non-rigid planet. p_m and r_m denote in these equations the amplitudes of nutation of a rigid planet. The first six amplification factors (also called transfer functions) are given in Table 2. The semi-annual prograde and ter-annual retrograde ranges of amplification have been used to compute (according to the two previous equations) the extend of the grey shaded boxes by multiplying them with the well-known rigid amplitude reported in Table 1.

One has to keep in mind however (as mentioned above) that these are "one sigma ranges". By allowing for three-sigma uncertainties on the interior structure parameters, the range of possible FCN periods is significantly broader and it includes the 230d forcing period (resonance).

[3] Konopliv et al. (2016) multiplied their formal errors by 15 mostly to account for systematics and because the data have not been whitened.

Table 2
Ranges of nutation amplification factors (unit-less) assuming $T_{FCN} \in [-280; -242]$ days as imposed by our current knowledge on Mars interior structure.

Period	Prograde amplification	Retrograde amplification
687 days	1.0113–1.0198	0.9737–0.9895
343.5 days	1.0147–1.0284	0.8674–0.9010
229 days	1.0167–1.0340	1.1187–2.0895
171.75 days	1.0181–1.0379	1.0612–1.2056
137.4 days	1.0190–1.0410	1.0483–1.1402
114.5 days	1.0200–1.0430	1.0430–1.1160

A deviation of the figure of the core from a hydrostatic shape could shift the FCN period closer to the forcing ter-annual period, implying larger signature of the liquid core in the nutation signal than considered here (Rivoldini et al., 2019).

Note that one can also assess the liquid core effect in the nutation signal by estimating the two parameters of the transfer function: the core momentum factor F and T_{FCN} (see for instance Folkner et al. (1997) or Le Maistre et al. (2012)). Fig. 5 shows the time evolution of both parameters. When estimating F and T_{FCN} instead of the nutation amplitudes (as above), the remaining parameters (precession, ΔLOD and lander position) can be estimated slightly more precisely (Le Maistre et al., 2012). This is mainly the result of the decreased correlation between the parameters. We however recommend to estimate the nutation amplitudes themselves, since observables depend linearly on them (in contrast to T_{FCN}) and can be estimated with confidence with a least square method. This is the reason why we focus on the p_2 and r_3 in the rest of the paper.

3. Mission duration and science operation calendar

This section discusses the effect of the mission duration on the precision we can expect on the estimated parameters. The impact of the actual period of science operation is also investigated here since LaRa science calendar is still uncertain because depending on the rover egress and instruments/solar panels deployments. We show in dark blue on Fig. 6 the ExoMars surface platform nominal mission of one Earth year starting from January 1st, 2021. In black is the extended mission. Note that the LaRa instrument lifetime guaranteed by design is at least 700 days. The impact of a launch delay is shown in cyan (thick curve). The beginning of this backup mission is postponed by 790 days with respect to the nominal mission. Such a delay corresponds to the Mars-Earth synodic period of revolution, necessary to renew the spatial configuration of the two planets. This period starts April 1st, 2023. The thin cyan curve corresponds to the thick cyan curve shifted by -790 days. It allows an easy comparison between the nominal and backup mission results. Similarly, the thick orange curve assumes a science phase of the ExoMars 2020 starting mid-July 2021 (i.e. 200 days after Jan. 1st, 2021), while the thin orange curve is identical but shifted by -200 days to ease the comparison.

As can be seen in Fig. 6, the first ~650 days of mission are very efficient for improving the nutation estimate precisions. After about 650 days, the precision on both p_2 and r_3 improves only marginally. We observe the same behaviour in the backup and delayed scenarios where the slope of the curves strongly reduces after about 650 days (i.e. about the fundamental period of one Martian year), making the subsequent measurements less powerful. The threshold (of 2–5 mas) in the formal error in the parameters that is reached then corresponds to the theoretical boundary of $\sqrt{2/N}(\sigma_{dop}/\Omega)$ equaling 3 mas, when the number of data points N is taken equal to 200 (i.e. one point twice per week during 100 weeks), and the numerical values of the Mars rotation rate (i.e. Ω = 350.89198°/day) and the LaRa measurements quality level (i.e. σ_{dop} = 3mHz at 60s integration time) are considered.

Finally, there is a small but noticeable difference between the black, cyan curves and the orange curve after 700 days of operation. This is likely due to the fact that the Earth declination is smaller than ~10°

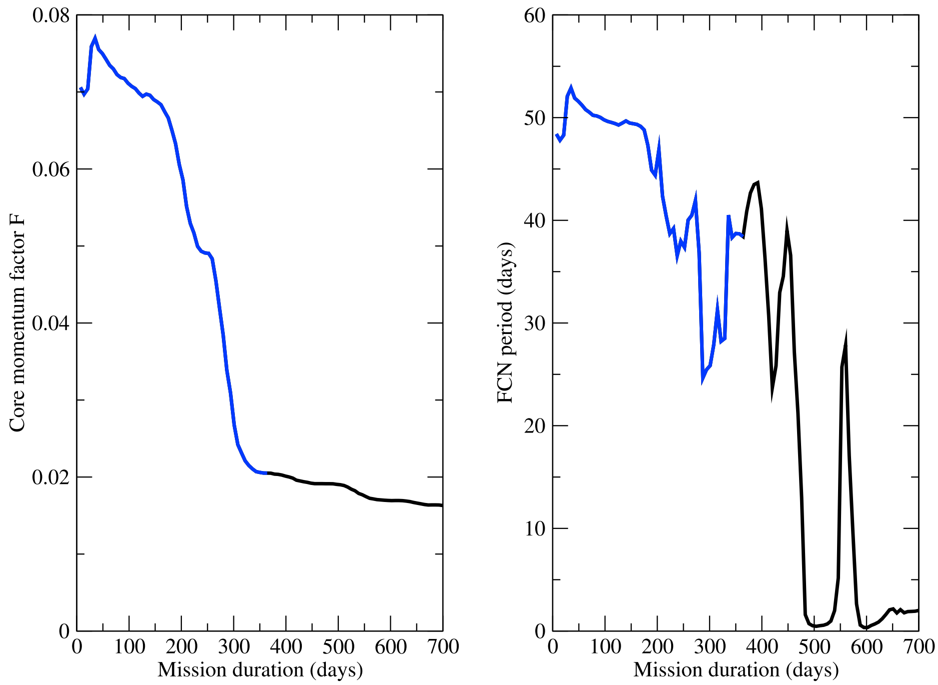

Fig. 5. Nominal scenario uncertainties of the alternative nutation parameters: the transfer function parameters *F* (core momentum factor, left panel) and the Free Core Nutation period (right panel).

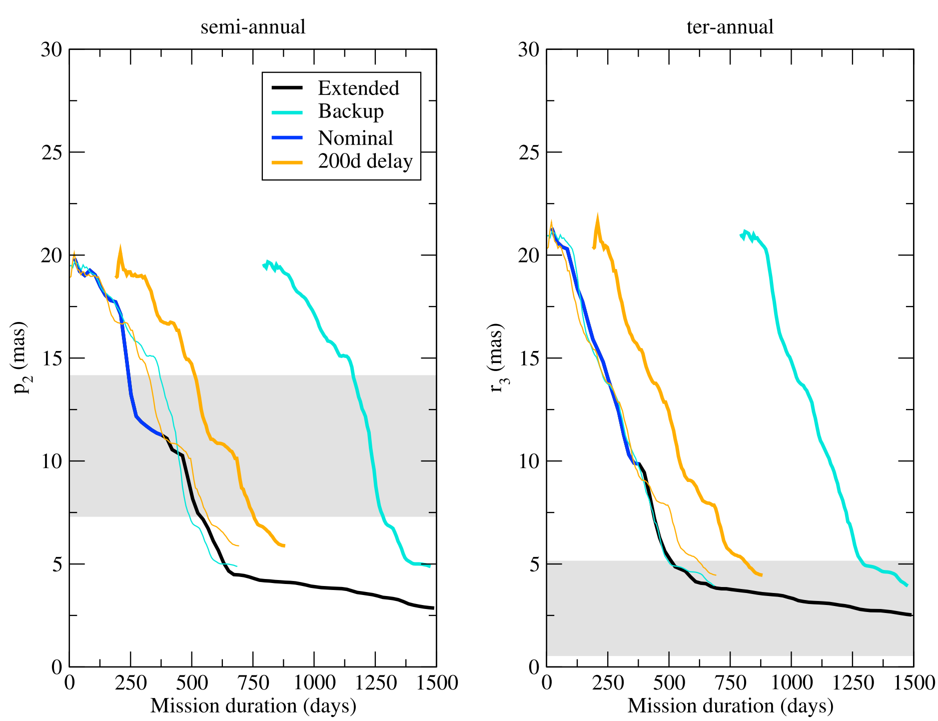

Fig. 6. Impact of the mission duration and science calendar on the nutation determination.

during a specially-long period of ~150 days between 600 and 750 days after Jan. 1st, 2021 during which the Doppler measurements are poorly sensitive to Mars spin axis motion in space at that time (Yseboodt et al., 2017).

4. Noise level

All measurements are affected by noise that is random signal from various origin, which is not the desired signal. This is also true in LaRa's Doppler link where the data quality for radio science is limited by non-signal disturbances. The latter are mainly due to instrumental noises (random errors introduced by the ground stations and LaRa itself), propagation noises (random frequency/phase fluctuations caused by refractive index fluctuations along the line of sight), or systematic errors (e.g. Asmar et al. (2005)).

The LaRa instrument (i.e. the transponder, the cables and the

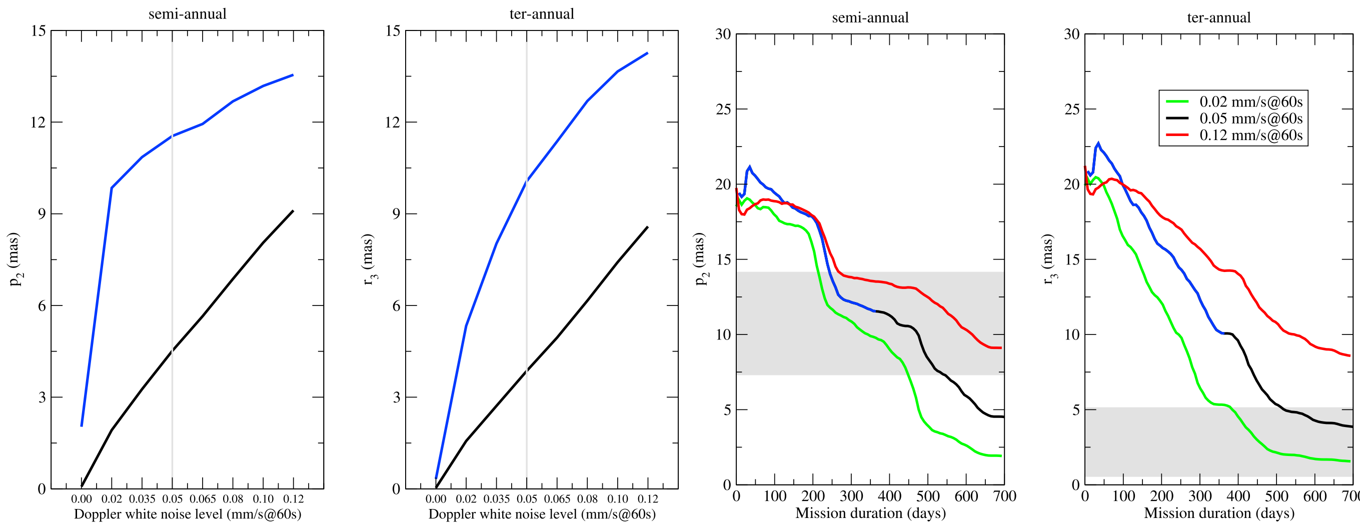

Fig. 7. Impact of the measurement noise on the nutation determination. On the left panels, the blue curves correspond to the uncertainties obtained after one Earth year of nominal mission, whereas the black curves correspond to the uncertainties obtained after 700 days of mission. (For interpretation of the references to color in this figure legend, the reader is referred to the Web version of this article.)

receiving (Rx) and transmitting (Tx) antennas) is designed to provide measurements affected by white noise of 0.02 mm/s at 60s of integration time (written hereafter 0.02 mm/s@60s) at the level of LaRa's transmitting antenna. This should ensure a noise level of the two-way (i.e. round trip) Doppler data at the ground station of about 0.05 mm/s@60s including all the error sources mentioned above (see details on the error budget in Dehant et al. (2019)). However, this noise level is not guaranteed because it is not fully controlled by the design of LaRa or the ground stations. This is the reason why we assess the impact of the measurements noise level on the nutation determination in this section of the paper.

4.1. White noise

We consider different level of white noise, varying from zero to 0.12 mm/s@60s. The case with zero noise is unrealistic and has to be considered as a case study. As expected and shown on Fig. 7, the impact of the noise on the nutation determination is major, the larger the noise, the larger the parameter estimate uncertainties. Looking at the black curves on left panels, corresponding to the uncertainties obtained after 700 days of mission, we see that the noise level linearly propagates to the parameter formal errors, which vary from zero to about 9 mas for both p_2 and r_3. Such a linear trend indicates that the parameters are poorly correlated with each others after 700 days of mission. This is not the case after only 365 days of mission where the non-linear blue curves indicates that the noise level plays a role in the parameters decorrelation.

In an ideal case with no noise at all, the determination of the ter-annual amplitude of nutation would be almost perfect (formal error close to zero) even after only one Earth year of mission. However, the lowest noise level is by design $\geq$0.02 mm/s@60s (green curves on right panels of Fig. 7). The green curves show the best we could have assuming the operation scenario described in Sec. 2.1. This ideal case would be especially useful for the determination of r_3 as suggested by the rightmost panel of Fig. 7. It is to mention that the typical noise of X-band data provided by orbiter is five times lower than our nominal 0.05 mm/s for similar 60s integration time (e.g. Zuber et al. (2007)). The nominal 0.05 mm/s noise level would better correspond to the level of orbiters X-band Doppler signal integrated over 10s. This suggests that the LaRa measurement noise could actually be somewhere between 0.02 and 0.05 mm/s@60s.

The red curves in Fig. 7 right panels correspond to the uncertainties obtained with 0.12 mm/s@60s. This level of noise is considered to be an upper limit, which won't be exceeded. As we can see on the graphs, even such an unlikely worst case would allow to detect the liquid core contribution in the semi-annual prograde amplitude.

4.2. Coloured noise

Interplanetary missions are also affected by coloured noises like those introduced by the Solar plasma and by the Earth troposphere and ionosphere. Solar plasma dominates at low SEP angles while fluctuations in the Earth troposphere are usually the dominant noise source of the Doppler data acquired elsewhere. This lower part of the atmosphere of the Earth strongly perturbs the propagation of an electromagnetic wave as shown on Fig. 8a, where the non-corrected Doppler residual of *Opportunity*[4] is plotted as a function of the radio signal elevation (α_e) in the sky of the DSN stations.

The troposphere contains both dry air and water vapor. The mixing ratio of dry-air constituents remains nearly constant in time while the water vapor content fluctuates widely as it depends on the local weather conditions. The dry (or hydrostatic) perturbation at the stations location can be accurately computed based on reliable surface pressure and temperature data since the laws of temperature and pressure decreasing with altitude are well known. The wet modeled component is much less reliable than the hydrostatic one because of the high spatial and temporal variability of the water vapor. In principle, it can be corrected for by using GNSS reconstruction of the local water vapor content or by using water vapor radiometer data. These corrections are not perfect and there is a remaining contribution of the troposphere after applying model predicted corrections. Such a residual tropospheric effect is shown on Fig. 8b and mostly corresponds to the wet tropospheric mis-modeling. Even after correction, a clear signature of propagation delays in the Earth atmosphere is still observed in the Doppler residuals (Fig. 8b exhibits a clear dependence to α_e that could also be partly induced by the Earth ionosphere) at a level of 3.8 mHz in RMS (Root Mean Square). This corresponds to about 0.07 mm/s in X-band. This is still above the 0.05 mm/s noise level target by LaRa, suggesting that additional calibration efforts are needed to better correct for Earth atmosphere perturbations.

Fig. 9 shows the impact on the nutation determination of the Earth

[4] Opportunity data acquired during the radio-science campaign of 2012 (Kuchynka et al., 2014).

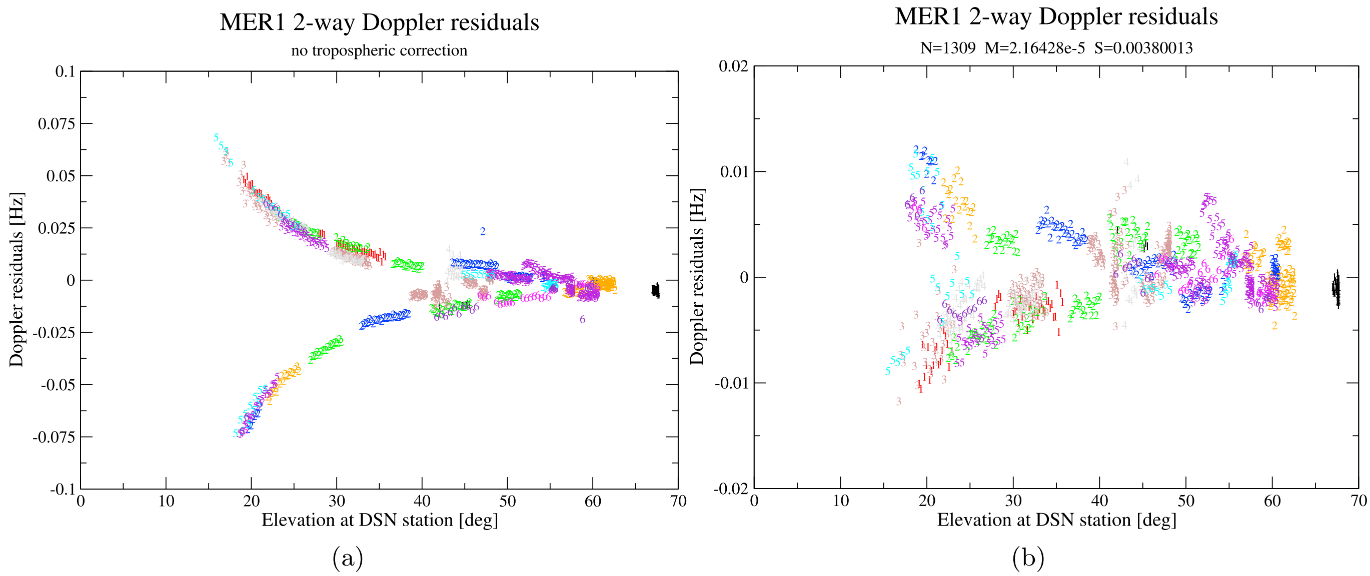

Fig. 8. Earth tropospheric signature in the Doppler residual of *Opportunity* as a function of the radio signal elevation in the sky of the DSN stations (α_e) before correction (a) and after correction (b). Each DSN station is reported with a special color and a number corresponding to the tens digit of its ID number, which is related to its location on Earth. (For interpretation of the references to color in this figure legend, the reader is referred to the Web version of this article).

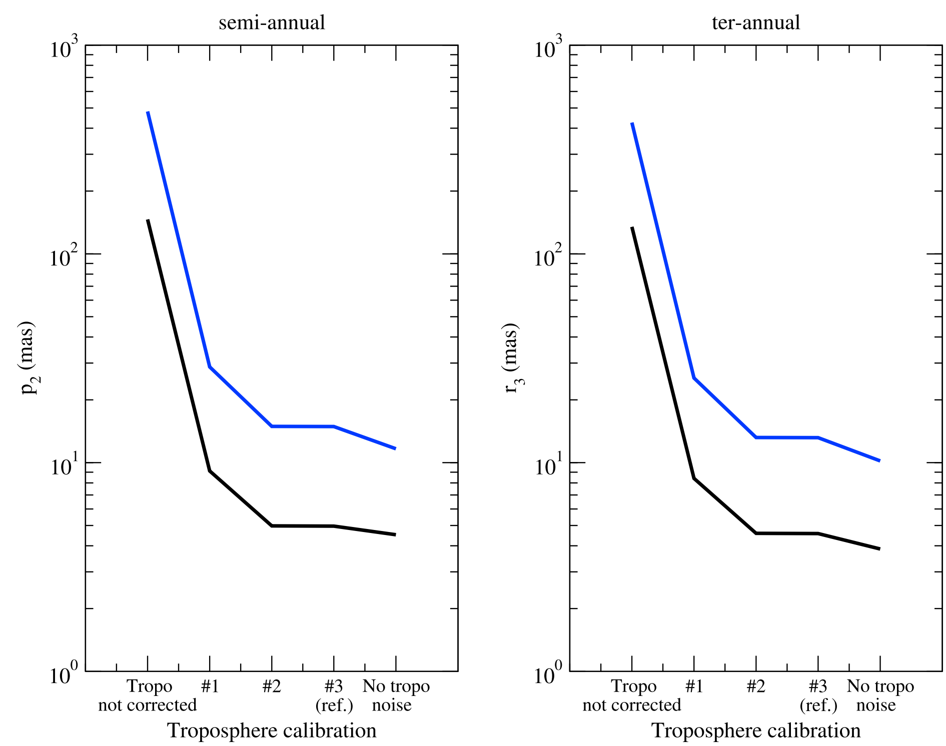

Fig. 9. Impact of troposphere noise on the nutation determination.

tropospheric noise. We see that not correcting the data would totally spoil the determination by increasing the uncertainties on p_2 and r_3 up to several hundreds of mas. This is of course not realistic as radio-science data are always troposphere calibrated. Nevertheless, as explained above, the wet troposphere component is difficult to model and will therefore always contaminate the data to a certain level. To characterise the effect of such mis-modeling, we generate synthetic data with a given troposphere model (#3: GPTMVF (Lagler et al., 2013)) and fit the nutation parameters using different troposphere models (#1: ECMWF, European Centre for Medium-Range Weather Forecasts numerical weather model data, and #2: GMFTP (e.g. Kouba (2009)). Fig. 10 shows the noise profiles considered in these simulations. We see on Fig. 9 that in the worst case tested here, the troposphere calibration errors would degrade the accuracy level of p_2 and r_3 by about 4 mas, which is significatif and confirms the necessity to carefully correct the data for Earth tropospheric noise.

Radio-waves propagation is also disturbed by the presence of plasma along the path (slightly slower in an ionised medium than in vacuum). Because Mars and the Earth are sometimes in conjunction, the LaRa signal periodically passes close to the Sun. The solar plasma, denser and

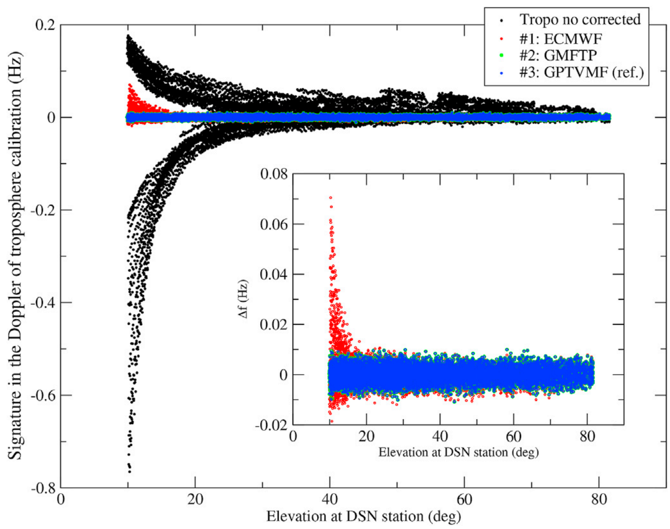

Fig. 10. Differences between LaRa Doppler measurements generated with a given troposphere model and those generated with the troposphere model of reference (#3: GPTMVF (Lagler et al., 2013)).

more active close to the Sun, strongly affects the radio signal at these time periods. Le Maistre (2013) used the Mars Express (MEX) Doppler data in X-band and S-band acquired between 2004 and 2011 in order to extract the plasma noise. Because the plasma effects on the signal are different for different frequencies, combining them allows to obtain the plasma noise. The latter is proportional to the differential Doppler $\Delta f^{xs} = \Delta f^{s} - \frac{3}{11}\Delta f^{x}$, which is shown on Fig. 11, according to

$$\Delta f_{ion}^{2w} = \frac{33}{112}\Delta f^{xs}\left(1 + \frac{880}{749}\right). \tag{4}$$

Le Maistre (2013) proposed a model allowing to compute the average plasma contribution to the Doppler data given the Sun-Earth-Probe (SEP) angle by plugging the differential Doppler (Δf^{xs}) computed with the model below into Eq. (4):

$$\Delta f_{mod}^{xs} = -2.526\alpha_{SEP}^{-4} + 4.777\alpha_{SEP}^{-2.5} - 0.001\alpha_{SEP}^{0.6} + 3.79e^{-12}\alpha_{SEP}^{4} + 0.024846. \tag{5}$$

The SEP angle has to be in degree and Δf_{mod}^{xs} is provided in Hertz. This model assumes the Doppler measurements integrated over 1s. Δf_{mod}^{xs} must therefore be rescaled according to the actual integration time t_c. Thanks to this empirical model, we are now able to cancel-out the strong disturbing signal shown in Fig. 11. This results in flattening the pre-fit RMS Doppler residuals at low-SEP-angle, preventing for bias in the nutation parameters estimates. However, the variance of the Doppler signal is not reduced by such a model. This is why LaRa real data acquired close to the solar conjunction will also be whitened according to the algorithm proposed by Mackenzie and Folkner (2006). This will allow us to affect the correct weight to each Doppler data point, providing in turn the proper uncertainties in the nutation parameters. The impact of the plasma noise on the nutation determination will be addressed in a future work. Nevertheless, the simulations presented in Sec. 7 (Fig. 19) below show that removing data points acquired at SEP $\leq 10°$-$15°$, i.e. when interplanetary plasma effect is dominant (see Fig. 11), does not prevent LaRa to reach its scientific goals.

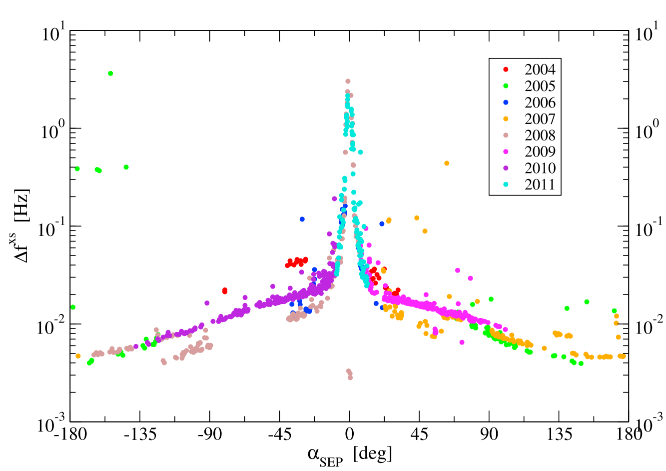

Fig. 11. Dual frequency data (Δf^{xs}) from MEX as a function of the SEP angle. Each point is the RMS of Δf^{xs} computed over one tracking pass.

5. Tracking pass characteristics

In this section we assess the impact on the nutation determination of the tracking pass characteristics, namely the duration (or length) of the tracking passes and their occurrence.

5.1. Length

As mentioned previously, the parameter uncertainties are inversely proportional to the square root of the number of data points. This means that lengthening the tracking pass duration will allow to estimate the parameters with a better precision. Here we quantify the impact of the tracking length on the nutation determination.

As expected, we see on Fig. 12 that the longer the tracking pass (i.e. the more we have data points because t_c is kept equal to 60s), the smaller the nutation estimate uncertainties. Generally speaking, doubling the tracking time with respect to the nominal 45 min will allow to gain something like 1-2 mas on the nutation estimate precision.Note that if there was no correlation between the different estimated parameters, the uncertainties obtained with a tracking pass duration T_{dur} could simply be predicted by rescaling the nominal scenario's uncertainties obtained with 45 min of tracking according to $\sigma_p(T_{dur}) = \sigma_p(45min)\sqrt{45/T_{dur}}$, assuming T_{dur} in minutes. The predictions obtained with this theoretical relation (dashed curves) are superimposed to the uncertainties computed with GINS (solid curves) in Fig. 12. As one can see, there is a very good agreement between the two for the estimates uncertainties obtained after 700 days of tracking (black curves), whereas the theoretical predictions are different when computed from the nominal obtained after 365 days of mission (blue curves). This tells us that one Earth year is not sufficient to annihilate the correlations between the parameters, whereas the latter are insignificant after 700 days. Moreover, such a low level of correlations after 700 days of mission, gives us confidence in the formal errors, which are fully representatives of the true errors made on each nutation parameter.

5.2. Occurrence

We test now the impact of the tracking occurrence on the determination of the nutation. We mean by tracking occurrence, the frequency at which the LaRa tracking sessions are carried out. The nominal case considers a tracking twice a week, every 3.25 days. In this section we perform simulations to see if having tracking passes closer to each other in time, or on the contrary more distant in time, would affect the scientific return of LaRa. To do so, we pay attention to keep the total number of measurements constant by reducing the tracking passes length when reducing the duration between two passes and reciprocally by increasing the tracking length when increasing the time between two passes. We also take care of keeping similar Doppler geometry than for the nominal case (i.e. similar LOS elevation and azimuth).

Two different cases are considered. First, we generate Doppler data at a constant occurrence, i.e. with regular time interval between each

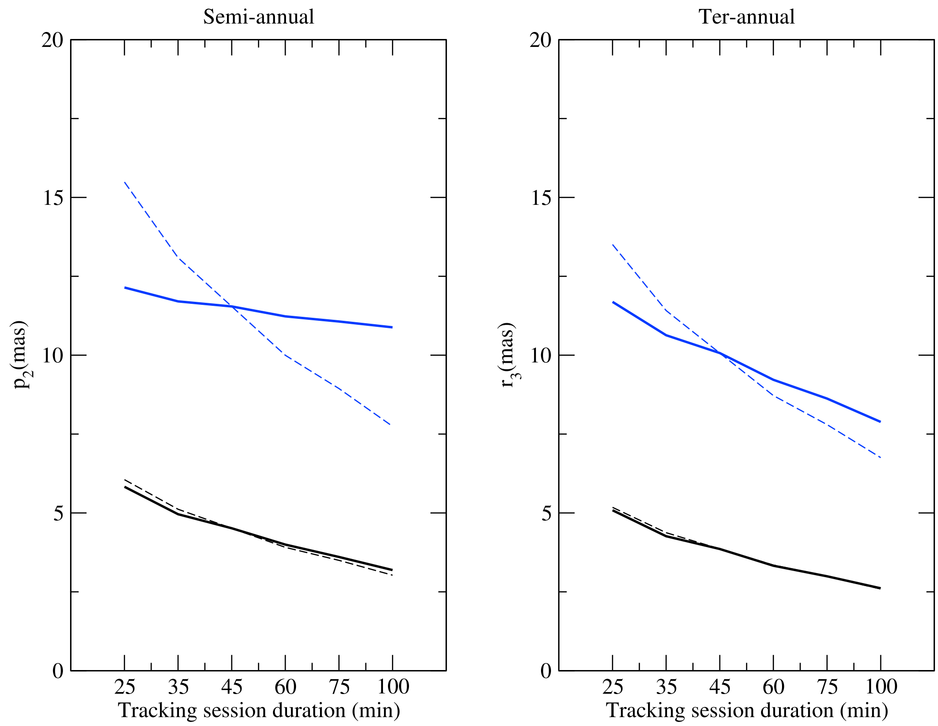

Fig. 12. Impact of tracking pass length on the nutation determination. Solid lines are the estimates uncertainties. Dashed lines are rescaled values (see details in the text).

tracking pass. Second we vary the time interval between two tracks.

5.2.1. *Regular time interval*

We run six different cases with tracking occurrences ranging from 30 min every 2.2 days to 189 min every 13.6 days. As shown on Fig. 13, whatever the tracking occurrence the nutation estimate uncertainties are always very similar to the one obtained in the nominal scenario. This is not really surprising given the periods of the signals of which we are estimating the amplitudes (i.e. several hundred days, so much longer than the longer interval of 13.6 days tested here). As a conclusion, the tracking occurrence is not a relevant quantity to account for in order to optimise the scientific return of LaRa. Nevertheless, the results shown

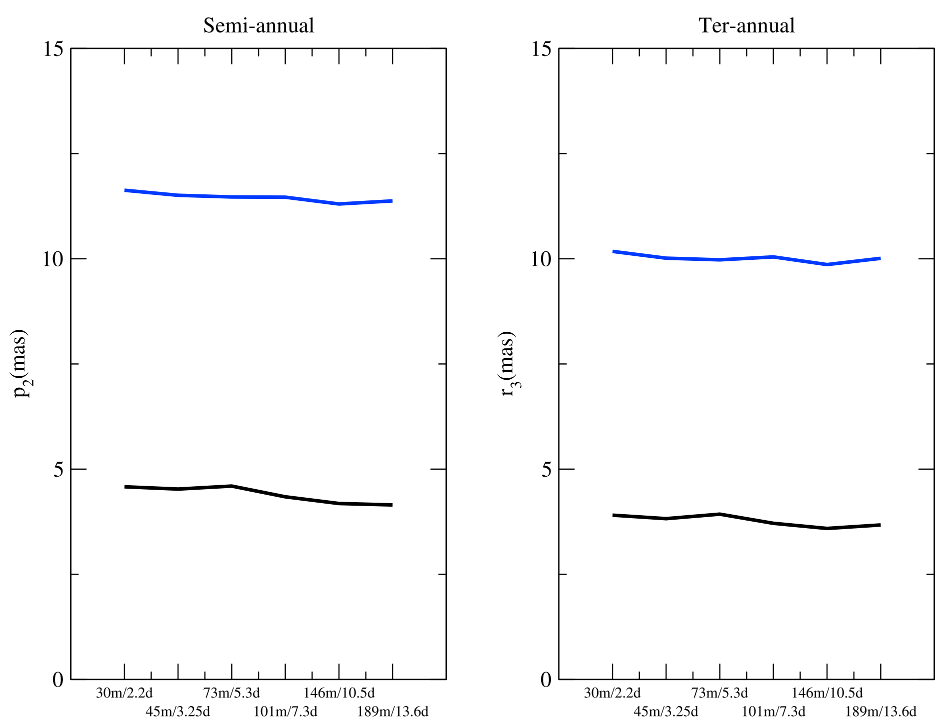

Fig. 13. Impact of the tracking occurrence with regular time interval on the determination of the nutation. x-label gives the tracking pass duration in minutes and the time interval in days between two tracking sessions.

here are of great interest for the definition of the LaRa operations, which depend on the ground station availabilities, the operation cost (fixed and variable), and the operations of the other scientific payloads.

5.2.2. Variable time interval

Same conclusions than for the case with regular time interval can be drawn when considering variable time interval between the tracking passes. Indeed, when we track LaRa during sessions of 45min separated by T_b days from the previous session and by T_a days from the following pass, with $T_b \neq T_a$, the precision with which nutation amplitudes can be determined does not change with respect to the nominal scenario (see Fig. 14).

6. Doppler geometry

This section focuses on the impact of the Doppler geometry on the determination of the nutation parameters. The two-way Doppler shift provided by the LaRa experiment is by definition related to the relative velocity of the lander and the Earth ground station according to the classical Doppler equation $\Delta f = 2 f_t v_r / c$, where f_t is LaRa's transmitted frequency and c the speed of light. This relative velocity (v_r) is a function of the lander position ($\overrightarrow{R}_L$) and velocity ($\overrightarrow{V}_L$) according to

$$v_r = \frac{(\overrightarrow{V}_{GS} - \overrightarrow{V}_L)\cdot(\overrightarrow{R}_{GS} - \overrightarrow{R}_L)}{\|\overrightarrow{R}_{GS} - \overrightarrow{R}_L\|}, \tag{6}$$

where $\overrightarrow{R}_{GS}$ is the position of the ground station in space and $\overrightarrow{V}_{GS}$, its velocity. Due to the projection (modeled by the scalar product) onto the LOS (modeled by the vector $\overrightarrow{R}_{GS} - \overrightarrow{R}_L$), the Doppler measurements do not contain the whole information on the lander three-dimension velocity and therefore do not contain the entire information on the nutation parameters either. The result of this projection is what we call the "Doppler geometry". This is an important quantity governing LaRa's measurements sensitivity to the MOP and therefore limiting their determination. Beside the data timing, three operational parameters basically control the Doppler geometry: the LOS elevation, the LOS azimuth and the lander latitude. The impact of those three parameters is assessed in the following subsections.

6.1. Line-of-sight elevation

Because the Earth trajectory in the lander sky is quasi identical from one day to the other, the Doppler geometry provided by a direct-to-Earth (DTE) radio link like the one of LaRa is not optimal for the MOP determination. Such a weakness is even accentuated in the case of LaRa, which proposed monopole antennas with fixed radiation pattern with respect to the local horizon (Dehant et al., 2019). The LaRa antennas bore sight (i.e. maximum gain direction) is between 35 and 45° of elevation (Dehant et al., 2019). Here we assess the impact of such a limited range of elevations on the nutation determination. We also test if another range of elevation would be more favorable to the determination of the nutation amplitudes.

Fig. 15 left panels show the nutation parameters uncertainties as a function of the LOS elevation. Generally speaking, we see that the nominal case with the LOS elevation ranging between 35° and 45° of elevation provides the best nutation estimates, except if the parameter fit is performed with measurements acquired within a large range of elevation (case "all"), which can be hard to achieve with the LaRa low gain antenna pattern. High LOS elevation solutions provide worst geometry to determine the nutation. Dashed black curve in Fig. 15 left panels are the 700d solutions rescaled with same data point number as nominal. This confirms that middle elevation angles are best suited for nutation amplitudes determination after 700 days operations (when parameter correlations are low). Fig. 15 right panels show that the two ranges around the nominal would provide similar results for r_3 and slightly less precise estimates of p_2. This gives us confidence on the ability of LaRa to achieve its science objectives even if we have to track outside the nominal 35-45° elevation range for programmatic reasons for instance. It also reinforces the LaRa antenna specifications we imposed to

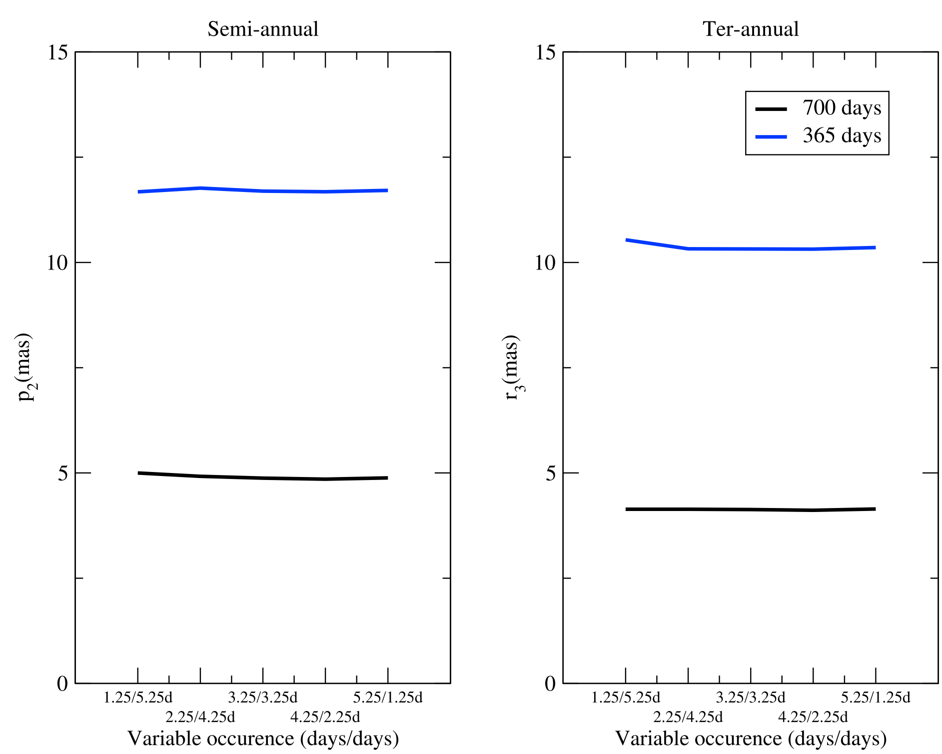

Fig. 14. Impact of the tracking occurrence with variable time interval on the determination of the nutation. x-label gives the time interval in days between preceding and succeeding tracking sessions (T_b/T_a).

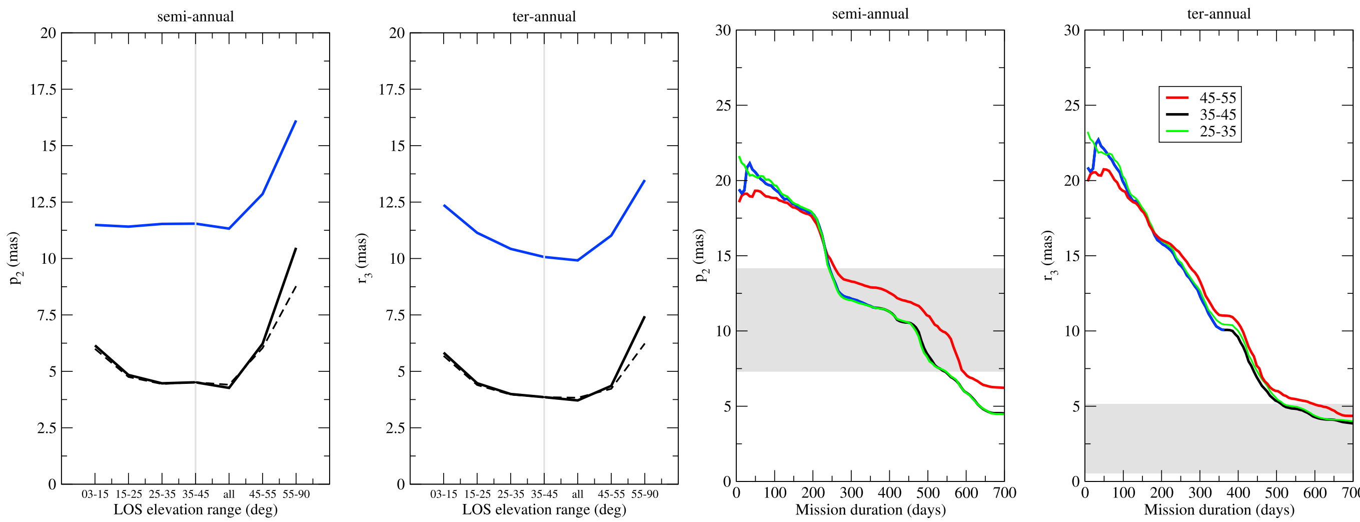

Fig. 15. Impact of the LOS elevation on the nutation determination.

industry to forced them to design antennas with maximum gain within 35-45° elevation (Dehant et al., 2019).

6.2. Line-of-sight azimuth

LaRa antenna lobes are omnidirectional in term of azimuth (i.e. almost the same gain whatever the azimuthal direction of the LOS during the tracking). This characteristic makes the design of LaRa monopole antennas pretty challenging because it limits the radiated power and thus the level of maximum gain. Such a characteristic is imposed by the attitude of the Russian platform, which is not controlled during landing (actual orientation after landing is unknown and unpredictable) as was the InSight spacecraft. As a consequence, we must be able to communicate with LaRa in every azimuth direction with the same performance. This weakness eventually appears to be a strength of LaRa with respect to InSight/RISE for instance, which has two directional medium-gain horn antennas with patterns limited in azimuth (Folkner et al., 2018). This is indeed what can be concluded from the simulations performed in this section. Here, in addition to the nominal case (WEN) for which the LOS azimuth direction switches from West to East, and reciprocally, every pass, we create six other sets of data. One consists of data acquired from East direction only (EO), one from West direction only (WO), two sets switch from East to West, and reciprocally, every six months (EW6 and WE6) and two others switch from East to West, and reciprocally, every month (EW1 and WE1). The last four cases are illustrated on Fig. 16.

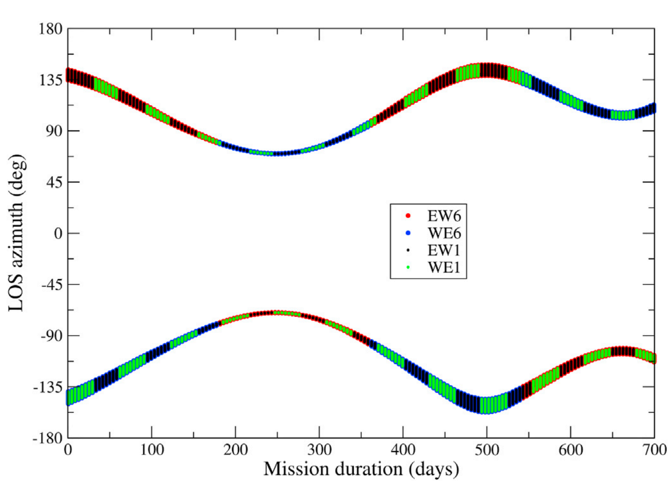

Fig. 16. LOS azimuth distribution of four different dataset considered here as a function of the mission duration. EW and WE means East-West and West-East respectively, while the subsequent number indicates the time in months during which the azimuthal configuration is maintained before switching (i.e. before going from eastward to westward LOS direction, and reciprocally).

Fig. 17 shows the strong impact of using data acquired from various LOS azimuth directions on the nutation estimates uncertainties. The more often we switch from East to West or West to East, the smaller are the uncertainties. Tracking from only one side of the lander during six consecutive months (as could have been the case for InSight/RISE[5] in case of an off-nominal orientation of the lander or could happen in case of failure of one antenna (Peters et al., 2019)) provides solutions twice less precise than LaRa's nominal case (WEN) of alternate tracking between eastward and westward LOS direction from one pass to the other. The repeatability of the Doppler geometry is shown here to limit the parameter estimation precision level.

6.3. Lander latitude

Until recently, there were still two landing site candidates for ExoMars 2020: the baseline, Oxia Planum, and the backup site, Mawrth Vallis. The former is the one finally selected by the science team in Nov. 2018. It is the one used in our nominal scenario. The latter is a bit higher in latitude with coordinates: 342° East, 22° North, 0 (assumed) km. As one can see on Fig. 18, the two landing sites offer similar nutation estimates, with a slightly degraded precision for the backup site as expected (Yseboodt et al., 2017). It is worth to mention here that the longitude of the lander has absolutely no impacts on the parameters determination because the rotation period of Mars (24.6 h) is very small with respect to the long-period (hundreds of days) signals of which we estimate the amplitudes.

7. Blackout periods

There will be blackout periods in the two-sessions-per-week tracking of LaRa. First during the solar conjunctions, when the plasma noise largely and quite suddenly (see Sec. 4.2) overwhelms any other valuable signals present in the data. The measurements acquired then are almost useless for the rotation determination. In addition, there is a chance of having blackout due to major dust storms, which may require the lander

[5] It must be mentioned that the InSight/RISE cadence of observation (one hour per day) is much larger than the LaRa one, which compensate for the repeatability limitation of the RISE experiment (see Peters et al. (2019)).

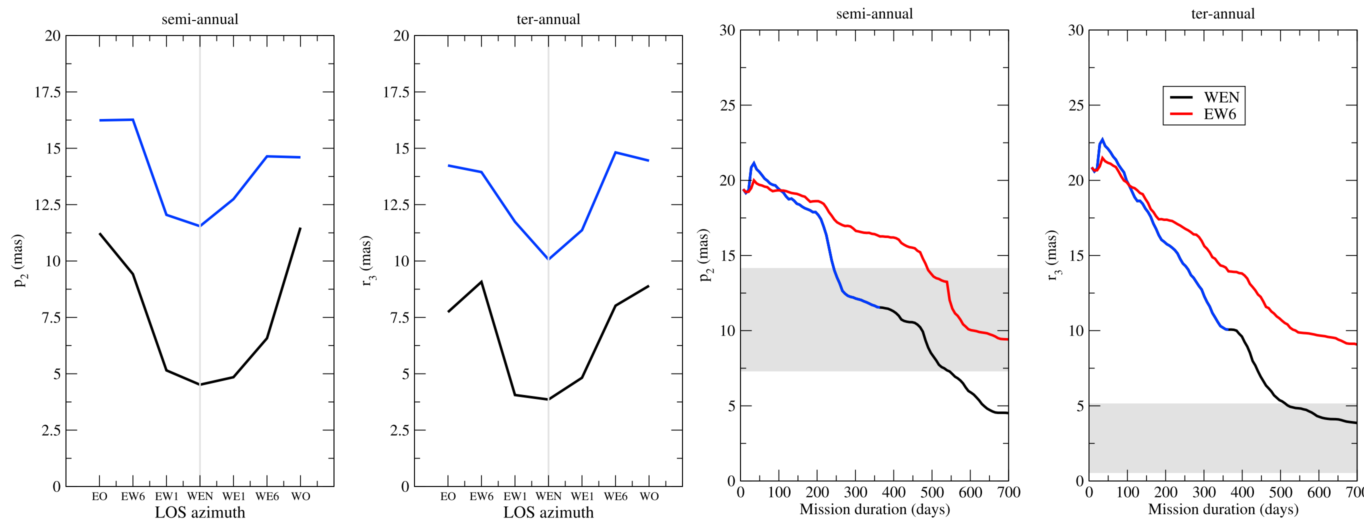

Fig. 17. Impact of the LOS azimuth direction on the nutation determination. WEN is the nominal case with alternating tracking between eastward and westward LOS direction from one pass to the other. See definition of the other cases in the text.

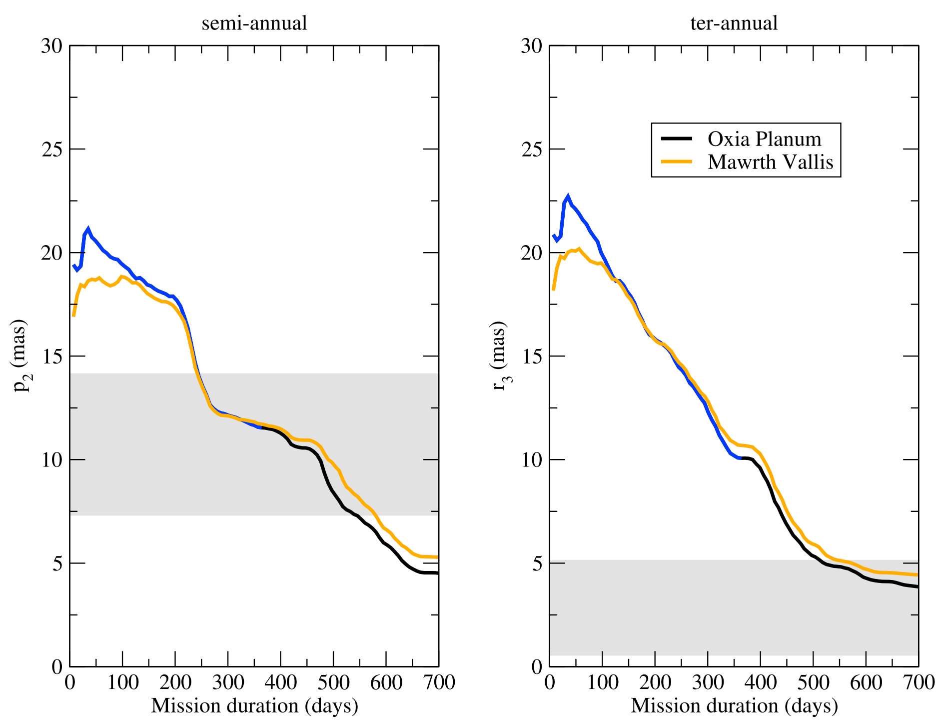

Fig. 18. Impact of the lander latitude on the nutation determination.

to be switched in save/sleeping mode for power saving for instance. Finally, the ground stations availability could also reduce the tracking opportunities. The ground stations case is discussed in Section 8, whereas the impact of the first two blackout causes is assessed hereafter.

7.1. Solar conjunction

As discussed in Section 4.2, and shown on Fig. 11, the plasma disturbing effect on the Doppler radically changes around $SEP_0 = 10^\circ - 15^\circ$, which may correspond to the solar corona boundary. For lower SEP than the limit angle SEP_0, the plasma noise increases with decreasing SEP at a rate 1000 times faster than for $SEP > SEP_0$. We thus expect that we will have to get rid of the data acquired below SEP_0. Here, we assess the impact on the nutation determination of removing a set of data acquired in a range of SEP angles where the plasma is dense and very turbulent, i.e. for SEP lower than SEP_0. We consider four cases shown on Fig. 19 where SEP_0 is set to 5°,10°,15° and 20°. Surprisingly, the removal of all data points acquired between 0 and $\pm 20^\circ$ of SEP has very little impact on the 700 days solutions (black curves). The impact is larger on the solutions computed after one year of mission (blue curves) as one could expect given the planets configuration, presenting a conjunction just before the end of the nominal mission (see for instance Fig. 1 of Yseboodt et al. (2017)). Fig. 20 shows in orange the time evolution of the nutation estimate uncertainties when data acquired at $SEP \leq 15^\circ$ are excluded due to high Solar plasma noise. We see that only few tracking passes after the blackout are needed to catch up on the nominal solutions.

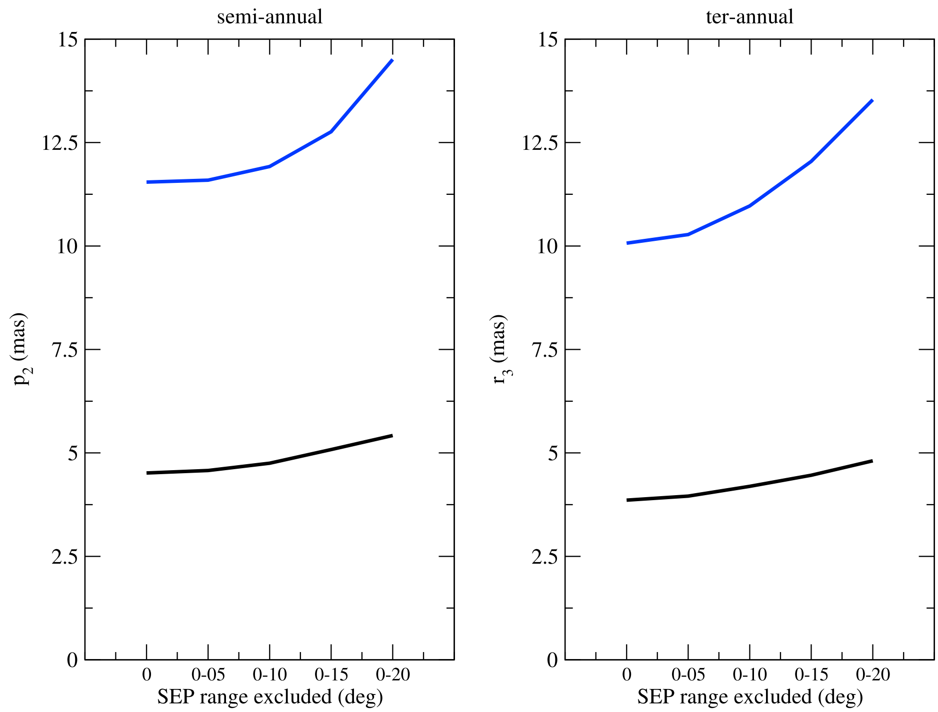

Fig. 19. Impact of the solar conjunction blackout on the nutation determination.

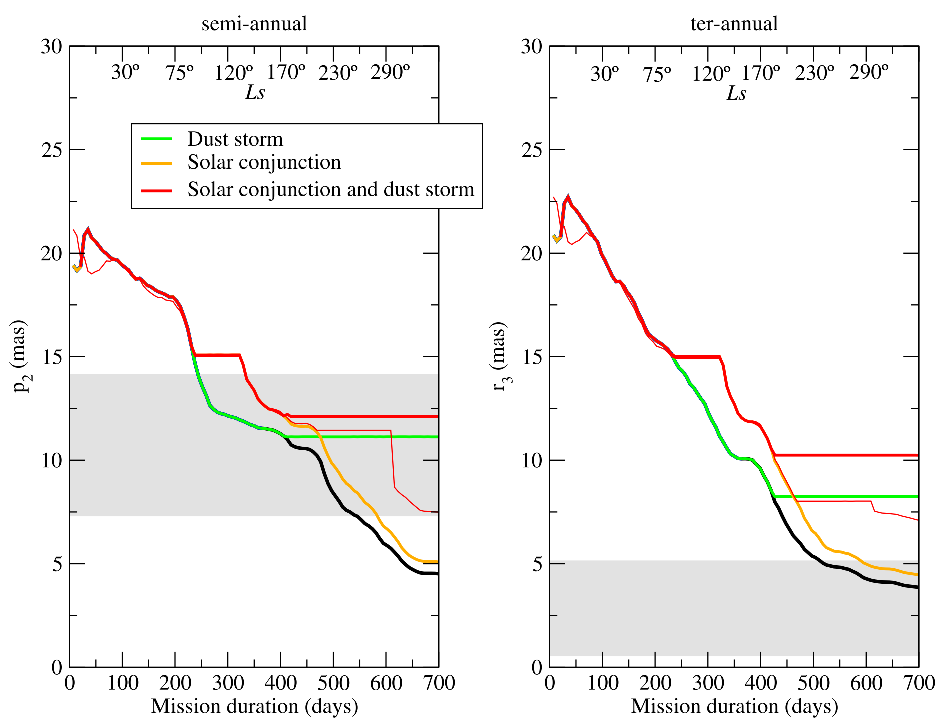

Fig. 20. Impact of blackout periods on the nutation determination. Red thick and thin curves include Solar conjunction followed by a 270-day and a 150-day dust storm blackout period, respectively. (For interpretation of the references to color in this figure legend, the reader is referred to the Web version of this article.)

7.2. Dust storms

Mars exhibits periodic dust storms distinguished from each other by their size (local, regional and global). The global dust storms encircling the whole planet can persist for many days and produce strong global effects on dust opacities, temperature etc. During such an event, it is likely that the platform will be switched in save mode and the science instruments (including LaRa) turned off. When and how long such a dust storm blackout can last? This is not precisely known since these events are difficult to predict. Even if the regional dust storms, which give birth to the global ones, can occur at almost any season, making the dust storm season somewhat arbitrary, it is generally admitted that dust storms most likely will occur around the solstice (at Mars Solar longitude $Ls = 270^{\circ}$, i.e. 570 days from 1st of January 2021). Following Beegle et al. (2007)

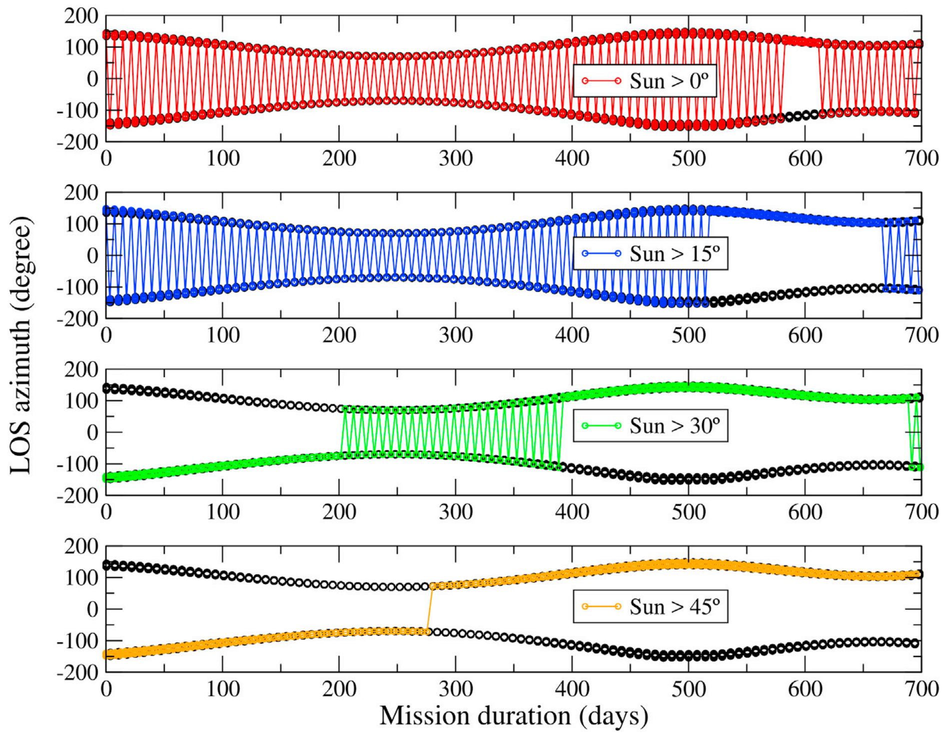

Fig. 21. Earth Line-Of-Sight (LOS) azimuth during tracking sessions. Black circles show nominal scenario while coloured circles show data coverage reduction induced by the (possible) necessity of having the Sun high enough to charge the SP batteries.

we considered here a dust storm period at $185^\circ < Ls < 350^\circ$. This corresponds to a blackout period of about 270 days starting right after the beginning of the extended mission. The consequences of such a rare but major event on the determination of the nutation are shown to be dramatic on Fig. 20 (green curve), preventing to observe the liquid core contribution in r_3 and solely allowing to observe the contribution of a large liquid core in p_2. Superimposed with the Solar conjunction, the impact is even worst as shown in red on Fig. 20. Nevertheless, as soon as the tracking is recovered the uncertainties decrease again and sometimes at a faster rate, as illustrated by the red thin curve of the left panel of Fig. 20 corresponding to p_2 uncertainty time evolution for a shorter 150-day dust storm scenario.

7.3. Power availability

The ExoMars 2020 surface platform is powered by solar panels, which drives the spacecraft activities schedule. The maximum power available during the SP surface operations should not exceed 120 W during days and 25 W during nights. LaRa consumes 40 W when turned ON, forcing day-time operations only. Due to the relative motion of Earth, Mars and the Sun, the Sunrise sometimes happens when Earth is already 'high' in the lander's sky (up to 40° elevation) and some other times the Sunset happens when Earth is still 'high' in the lander's sky (also up to 40° elevation). Our reference scenario does not account for power issues, therefore some data points acquired when the Sun is not above the horizon are included. Since the nominal elevation range of the Earth during LaRa tracking is 35-45°, tracking during night is fortunately rare (see Fig. 21 top panel where black circles are day-and-night sessions while red circles are day-only sessions). This explains why allowing to tracking only during the day does not degrade much the nutation determination (see Fig. 22). Assuming worse-case scenarios where LaRa operations would not be allowed while the Sun is not above a given elevation threshold (for example: at least one hour[6] of insolation could be needed for the spacecraft to recover nominal power and operate LaRa), we show in Fig. 21 what would be the impact for the tracking configuration. Generally speaking, we see that power issues could significantly reduce the tracking opportunities, limiting the azimuth allowed during tracking, which can have strong impact on the nutation determination as shown in Sec. 6.2. According to Fig. 22, which shows the impact on the nutation determination, one can finally conclude that waiting for the Sun to be at minimum 15° of elevation above the lander is still acceptable, but higher elevation threshold would strongly reduce the science return of LaRa.

8. Ground stations network

LaRa experiment requires the use of giant ground stations on Earth to transmit a radio-signal to LaRa and listen to the signal coherently sent back by LaRa. The ground segment of the experiment is the American Deep Space Network (DSN). However, the European ESTRACK network and the Russian network might also be used. DSN has two main advantages with respect to the others. First, it has high-performance-70 m antennas, whereas ESTRACK antennas have 35 m antennas only,[7] which do not always allow to close the link-budget (see Dehant et al. (2019)) and Russian 64 m antennas need to be upgraded to allow two-way tracking operations. Second, the DSN antennas are well distributed in longitude and latitude all over the world such that LaRa can always be tracked when it faces the Earth. This is also the case of the ESTRACK network, but Russian stations[8] are all placed in the north hemisphere in a

[6] Note that the Earth/Sun elevation varies of about 15° in one hour.

[7] It is interesting to note that ESA is currently transforming the Italian Sardinia radio telescope (64 m) into a full Tracking, Telemetry and Command (TTC) antenna for deep space mission. The latter should be operational before ExoMars 2020 arrival at Mars and would be perfectly suited for the LaRa experiment.

[8] Bear Lakes and Kalyazin stations (very close to each other at about 55° of North latitude and 37° of East longitude) could in theory be involved in the LaRa ground support, but getting the other two, Yevpatoria and Ussuriisk, is unlikely for political reasons.

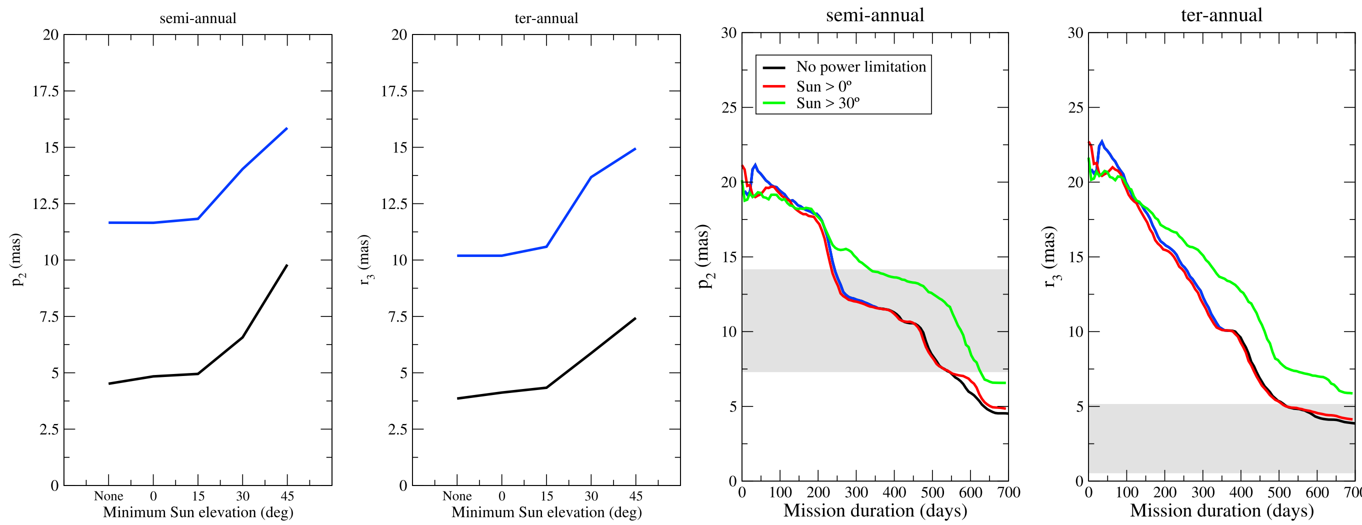

Fig. 22. Impact of blackout periods due to power availability on the nutation determination.

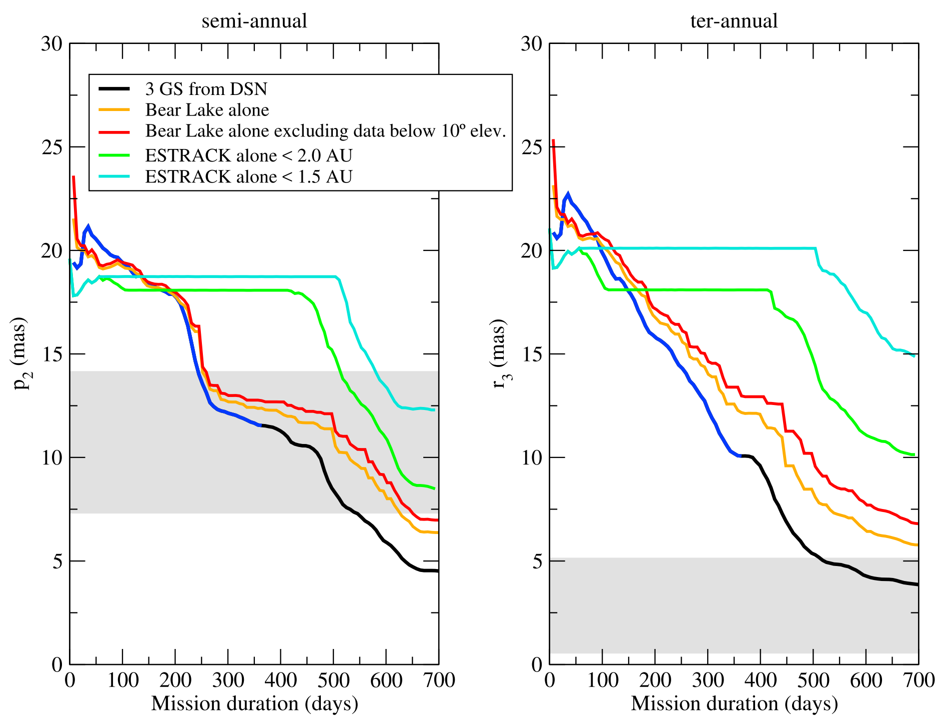

Fig. 23. Impact of the Ground Stations (GS) network on the nutation determination.

limited range of longitudes of about 90°.

We take a look here at the impact of the ground stations used to track LaRa on the nutation determination. As suggested in the previous sections, having only one station will reduce the opportunities to track LaRa and thus will create small but frequent blackout periods (i.e. when tracking pass of 45-min nominal duration is not alway possible) that could have bad influence on the MOP determination. Fortunately, as shown on Fig. 23, the nutation estimates uncertainties obtained with the full Russian network are similar to that obtained with the DSN network used in the nominal scenario. Moreover, the use of Bear Lakes alone still enables the detection of the liquid core contribution on p_2 but prevents to observe its contribution in r_3. Note that excluding the Doppler data acquired at elevation lower than 10° in the sky of the Bear Lakes station (typical to avoid large atmospheric perturbations) does not affect significantly the parameter estimate precisions (red curve compared to orange curve).More problematic are the blackout periods induced by the inability of LaRa receiver to lock on an uplink signal of too low input power (i.e. < -140dBm). As explained by Dehant et al. (2019), such a situation happens with ESTRACK stations when the Earth-Mars distance is larger than 1.5-2 AU (astronomical units). Therefore, the inability to always close the link budget with ESTRACK in closed-loop mode precludes the detection of the liquid core contribution in r_3, and induces major degradations in the estimates precision in general (see Fig. 23).

9. LaRa's distinct Rx and Tx antennas

Differently from all spacecraft radio-science instruments and telecom systems, the LaRa instrument is the only one having distinct receiving (Rx) and transmitting (Tx) antennas. Actually, to reduce the risks related to failure of the transmitting chain of LaRa (further details in Dehant

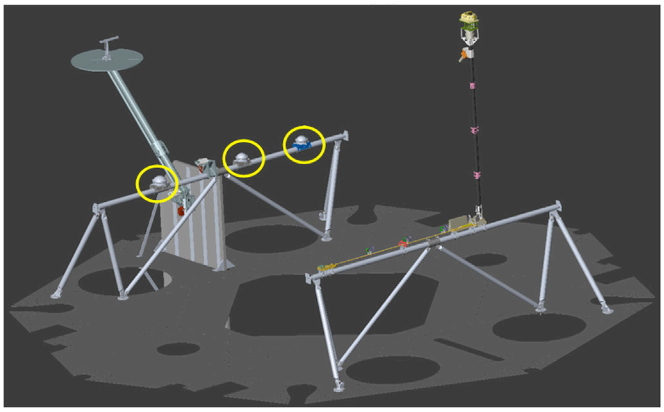

Fig. 24. LaRa one-Rx (rightmost) and two-Tx antennas aligned on a boom 80 cm above the deck of the ExoMars 2020 Surface Platform.

et al. (2019)), the latter has been made redundant with two Tx antennas, as shown on Fig. 24. Only one of the two Tx will be used at a time, but none of the Tx is superimposed with Rx. Since LaRa is designed to accurately monitor the motion in the inertial space of a point fixed to the Martian surface, having two separated antennas can introduce confusion and misleading interpretation of the measurements in terms of nutation determination for instance. The integration of LaRa antennas on the SP allows having them apart from each other by maybe more than 1 m (but for sure less than 2 m) along a horizontal boom (see Fig. 24). Such a distance can be totally insignificant in the Doppler if the boom is alined with a meridian of Mars, for the exact same reasons that LaRa direct-to-Earth Doppler data are not sensitive to the z (along spin axis) coordinate of the lander (see details in Le Maistre et al. (2012)). However, if the actual orientation of the lander is such that this boom is parallel to the equator (East-West oriented), then the signature in the Doppler measurements of the Rx-Tx distance will be significantly large. A 2-m distance in longitude between Rx and Tx has a signature of up to 0.06 mm s^{-1} (see black curve Fig. 25), which is slightly larger than the Doppler noise when integrating over 60s. This signature decreases to 0.02 mm s^{-1} for a 2-m distance in latitude (see red curve Fig. 25). This is the reason why the Rx-Tx distance is accounted for in GINS when computing the theoretical Doppler measurements that will be compared in a least square sense to the forthcoming real LaRa measurements. The not-modeled Rx-Tx distance is shown in Fig. 26 not to prevent the proper nutation determination. Indeed, the true errors (dots) roughly remain

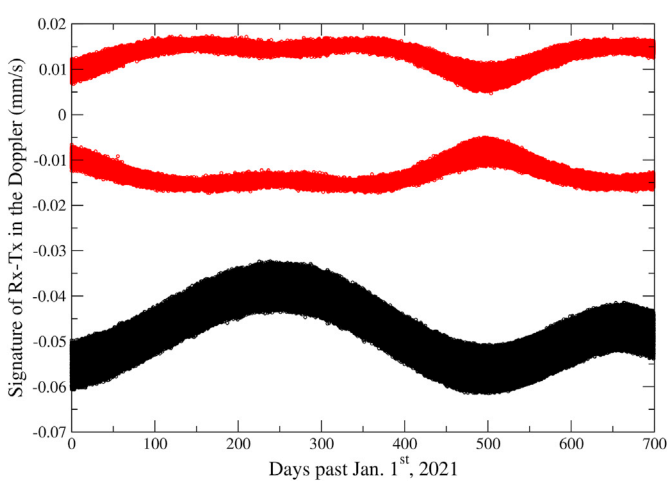

Fig. 25. Signature over 700 days in LaRa's Doppler measurements of the distincts Rx and Tx antennas, separated by 2 m in longitude (black) or 2 m in latitude (red). (For interpretation of the references to color in this figure legend, the reader is referred to the Web version of this article).

lower than the formal errors (solid lines), which means that no noticeable bias is introduced in the nutation estimates when 2 m separates Rx and Tx on the boom, even when the boom is East-West oriented. This is because the signatures of the Rx-Tx distance in the Doppler differs from the one of the nutation signal. Nevertheless, it is recommended to precisely know the actual orientation of the ExoMars 2020 surface platform to accurately compute the theoretical Doppler measurements of LaRa.

10. Two landers

Assuming the InSight mission is still functional at ExoMars 2020 arrival, then we will have two radio-science experiments operating at Mars in the same time. Realistic simulations of such a synergy are discussed in Peters et al. (2019), while here we investigate the effect on the nutation determination of a combination between two LaRa-like landers located at different longitudes and latitudes. In order to test the possible benefit of having two landers instead of one, we consider 22.5 min of tracking for each lander, keeping this way the same total number of data points as in the nominal case. Six second lander locations are considered, four are shifted in latitude (30° South, 15° South, at the equator or 15° North) with respect to LaRa nominal location and two are shifted in longitude (233° West or 73° East). As shown in Fig. 27 (left panels), the higher the latitude of the second lander, the larger are the uncertainties. Conversely, whatever the longitude of the lander, the nutation estimate uncertainties are very similar to the one obtained in the nominal scenario with only one lander. This leads us to conclude that having two landers instead of one (whether tracking is simultaneous or not) does not improve our ability to precisely determine the nutation amplitudes. This conclusion is correct for the nutation parameters, but does not apply for all MOPs (e.g. polar motion would definitely benefit from having a second set of observations acquired at high latitude).Although, two simultaneous radio-links would allow better removal of the Earth atmosphere noise in the data, given the respective location of InSight (135.62°E) and ExoMars 2020 (335.37°E), the only way to get simultaneous tracking would be to track both at very low elevation (i.e. $<$ 20°), which can not be done for LaRa at large Earth-Mars distance (due to link-budget limitation as discussed in Dehant et al. (2019)).

11. Conclusion

This paper provides a detailed view of the impact of operational and technical characteristics of the LaRa experiment on its ability to precisely determine the nutation amplitudes of Mars. As summarised in Fig. 28, we quantified the level of degradation or improvement with respect to a nominal scenario in the nutation estimates precision induced, among others, by the data noise level, the tracking pass duration and occurrence, the mission lifetime and science schedule, the radio signal elevation and azimuth in the lander sky, the blackout periods and the on-board power availability. These quantitative inputs can be used for the programmatic of radio-science experiments onboard a lander using direct-to-Earth Doppler measurements (like RISE on the InSight mission) with the objective of optimising the determination of the amplitudes of Mars nutation.

This study first confirmed the necessity to accumulate tracking data over at least one Martian year in order to annihilate the correlations between the Mars rotation parameters and optimise their determination. We compared different mission calendars, concluding that a science phase starting mid 2021 is not the best for the determination of the nutation of Mars because the Earth declination is small ($<$ 10°) during a specially-long period of ~ 150 days near the end of the one Martian year mission (i.e. end of year 2022). Such a disadvantage of the science calendar of the ExoMars 2020 mission should however not prevent LaRa from observing the liquid core contribution in the nutation signal.

Special attention must be paid to optimally calibrate the data since the measurement noise propagates in a on-to-one way on the parameters' uncertainty. In particular, we showed here that the discrepancy between

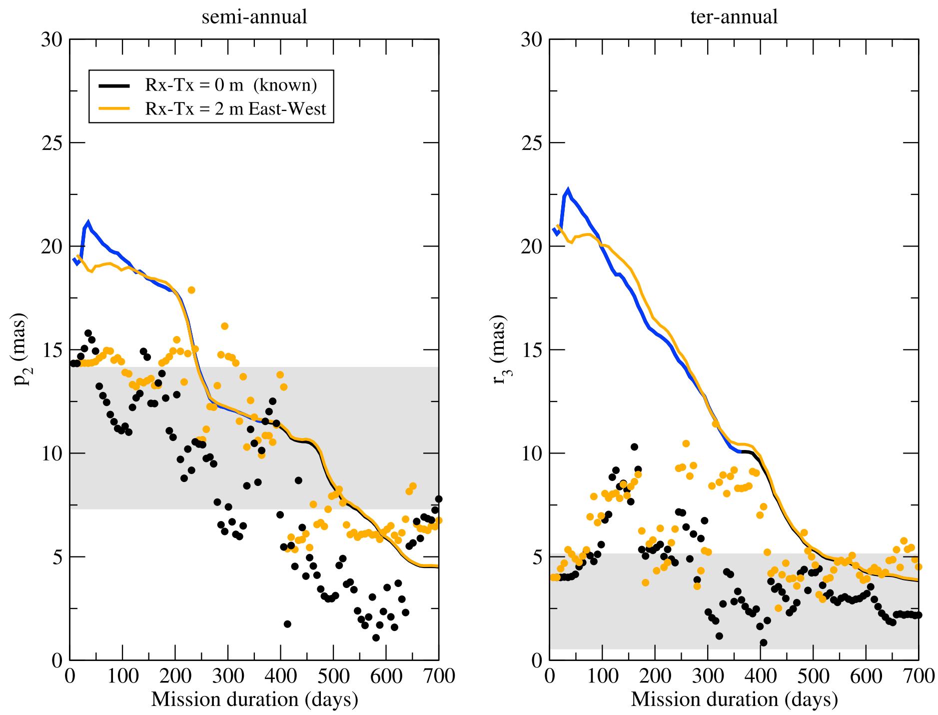

Fig. 26. Impact of a not-modeled difference in Rx and Tx antenna location on the determination of the nutation. Only the worst case with Rx and Tx separated by 2 m in longitude his considered here. Orange and black solid-circles are the absolute true errors made on the parameter estimates. They show that no significant bias is introduced by the Rx-Tx non-zero distance. (For interpretation of the references to color in this figure legend, the reader is referred to the Web version of this article).

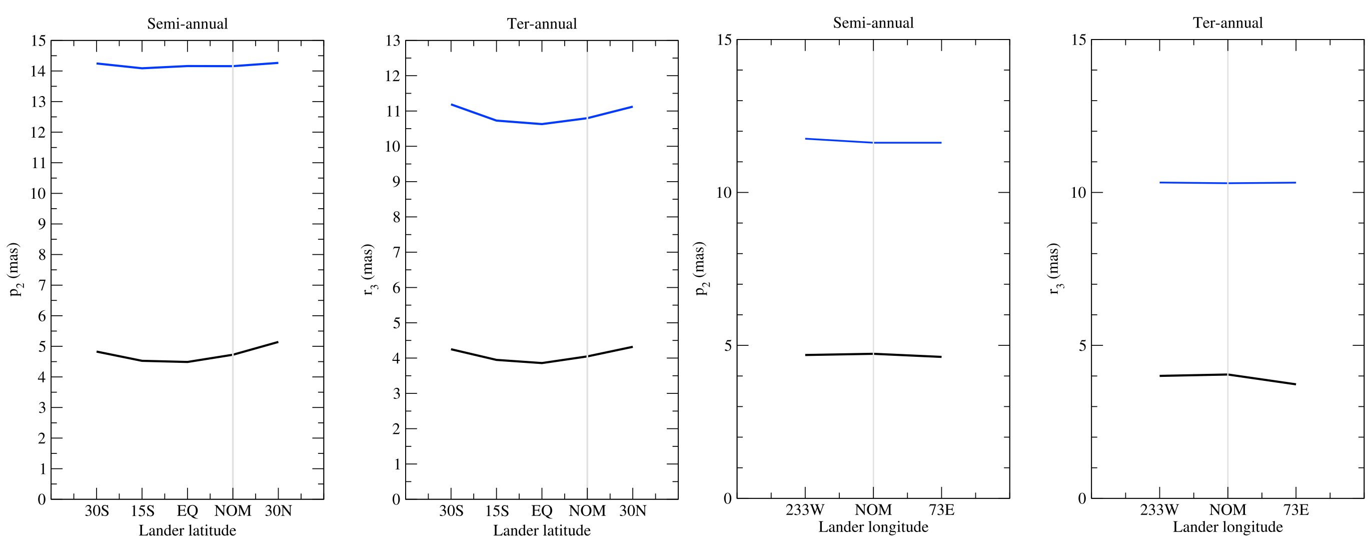

Fig. 27. Impact of two landers instead of one on the nutation determination. NOM is the reference obtained from one LaRa at 335.45° E, 18.20° N.

up-to-date Earth troposphere models can be responsible for a 4 mas degradation of the precision in the nutation determination, which is at the level of the liquid core signature in the nutation amplitudes.

We demonstrated that the tracking occurrence (i.e. the frequency at which the tracking sessions are carried out) is not a relevant quantity to optimise the science return of LaRa since short-time frequent tracking sessions give the same precision in the nutation determination than less frequent but longer tracking sessions, providing that the total amount of data points remains identical. This information is however of great interest for the definition of the experiment's operations, which depend on the ground station availabilities and operation cost (fixed and variable). On the contrary, the geometry of the radio path between the lander and the Earth is shown to be crucial for the science return of the experiment. It is in particular shown that operating LaRa when the Earth is at elevation around 40° in the lander sky is well suited for the determination of the nutation amplitudes, while alternance of Earth azimuth during tracking (i.e. one pass when Earth rises in the lander sky (Eastwards) followed by one pass when Earth sets (Westwards)) is mandatory to best fit the Mars rotation parameters.

We quantified the influence on the nutation determination of periods of blackout, during which no data are acquired, showing that solar conjunction blackout degradation can fairly well be absorbed while large dust storms blackout could strongly reduce the scientific return of LaRa if lasting too long. Additional periods of blackout could arise due to lack of power available on the surface platform. This study made us to conclude that waiting to operate LaRa for the Sun to be at minimum 15° of

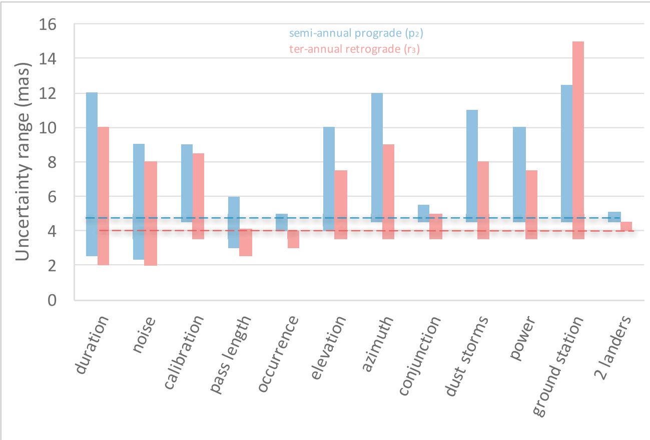

Fig. 28. Levels of improvement and degradation in the nutation determination for the different cases tested in this study. Nominal uncertainties in p_2 and r_3 correspond to dashed-horizontal blue and red lines, respectively. (For interpretation of the references to color in this figure legend, the reader is referred to the Web version of this article).

elevation above the lander is acceptable, but requiring higher elevation of the Sun would strongly reduce the science return of LaRa. Finally, the inability of LaRa receiver to lock on an uplink signal of too low input power (i.e. < -140dBm) could happen when the Earth-Mars distance is larger than 1.5–2 AU if 35 m dish antennas on Earth are used. Such a new kind of blackout periods would preclude the detection of the liquid core contribution in the nutation ter-annual signal, and induce major degradations in the MOP estimates precision in general. This led us to require DSN 70 m stations to track LaRa at long Earth-Mars distance.

The LaRa instrument has the specificity to have distinct and non-superimposed receiving (Rx) and transmitting (Tx) antennas. A 2-m distance in longitude between Rx and Tx has a signature of up to 0.06 mm s^{-1}, which decreases to 0.02 mm s^{-1} for a 2-m distance in latitude due to projection onto the line-of-sight. Although, the GINS software, especially developed to process forthcoming LaRa's data, accounts for the Rx-Tx distance in the elaboration of the theoretical Doppler observable, our study showed that no noticeable bias is introduced in the nutation estimates when the 2-m distance between Rx and Tx is not modeled, even when the Rx-Tx vector is East-West oriented.

Finally, having two LaRa operating at Mars simultaneously is shown here not to significantly improve our ability to precisely determine the nutation amplitudes if the total amount of data points is kept constant. This conclusion does not apply for all rotation parameters since polar motion would benefit from observations from a higher latitude spacecraft for instance. Note that the specific investigation on the advantage of having LaRa (ExoMars, 2020) after RISE (InSight) in the nutation determination and interior modeling is addressed in a compagnon paper (Peters et al., 2019).

It is worthwhile to eventually mention that the actual precision of the nutation parameters that will be achieved with LaRa could slightly deviate from those presented herein since the set of parameters and the strategy to determine them is still under study and will be optimised in a near future as will be the signal preprocessing (to reduce the data noise).

Declaration of competing interest

The authors declare that they have no known competing financial interests or personal relationships that could have appeared to influence the work reported in this paper.

Acknowledgments

This work was financially supported by the Belgian PRODEX program managed by the European Space Agency in collaboration with the Belgian Federal Science Policy Office. This study was supported by the French Space Agency (CNES) in Toulouse. The authors thank A. Rivoldini for providing inputs used to draw Fig. 1 and M. Yseboodt for her constructive proofreading.

Appendix A. Supplementary data

Supplementary data to this article can be found online at https://doi.org/10.1016/j.pss.2019.104766.

References

Asmar, S.W., Armstrong, J.W., Iess, L., Tortora, P., April 2005. Spacecraft Doppler tracking: noise budget and accuracy achievable in precision radio science observations. Radio Sci. 40, RS2001. https://doi.org/10.1029/2004RS003101.

Beegle, L.W., Wilson, M.G., Abilleira, F., Jordan, J.F., Wilson, G.R., August 2007. A concept for NASA's mars 2016 astrobiology field laboratory. Astrobiology 7, 545–577. https://doi.org/10.1089/ast.2007.0153.

Defraigne, P., Dehant, V., Pâquet, P., December 1995. Link between the retrograde-prograde nutations and nutations in obliquity and longitude. Celest. Mech. Dyn. Astron. 62, 363–376. https://doi.org/10.1007/BF00692286.

Dehant, V., Defraigne, P., Van Hoolst, T., January 2000. Computation of Mars' transfer functions for nutations, tides and surface loading. Phys. Earth Planet. Inter. 117, 385–395.

Dehant, V., Folkner, W., Renotte, E., Orban, D., Asmar, S., Balmino, G., Barriot, J.-P., Benoist, J., Biancale, R., Biele, J., Budnik, F., Burger, S., de Viron, O., Häusler, B., Karatekin, Ö., Le Maistre, S., Lognonné, P., Menvielle, M., Mitrovic, M., Pätzold, M., Rivoldini, A., Rosenblatt, P., Schubert, G., Spohn, T., Tortora, P., van Hoolst, T., Witasse, O., Yseboodt, M., July 2009. Lander radioscience for obtaining the rotation and orientation of Mars. Planet. Space Sci. 57, 1050–1067. https://doi.org/10.1016/j.pss.2008.08.009.

Dehant, V., Le Maistre, S., Rivoldini, A., Yseboodt, M., Rosenblatt, P., Van Hoolst, T., Mitrovic, M., Karatekin, Ö., Marty, J.C., Chicarro, A., 2011. Revealing mars' deep interior: future geodesy missions using radio links between landers, orbiters, and the earth. Planet. Space Sci. 59, 1069–1081. https://doi.org/10.1016/j.pss.2010.03.014. ISSN 0032-0633.

Dehant, V., Le Maistre, S., Baland, R.-M., Bergeot, N., Karatekin, Ö., Péters, M.-J., Rivoldini, A., Ruiz Lozano, L., Temel, O., Van Hoolst, T., Yseboodt, M., Mitrovic, M., Kosov, A., Valenta, V., Thomassen, L., Karki, S., Al Khalifeh, K., Craeye, C., Gurvits, L.I., Marty, J.C., Asmar, S., Folkner, W., the LaRa team, 2020. The radioscience LaRa instrument onboard ExoMars 2020 to investigate the rotation and interior of Mars. Planetary and Sapce Science 180, 104776. https://doi.org/10.1016/j.pss.2019.104776.

Folkner, W.M., Kahn, R.D., Preston, R.A., Yoder, C.F., Standish, E.M., Williams, J.G., Edwards, C.D., Hellings, R.W., Eubanks, T.M., Bills, B.G., February 1997. Mars dynamics from earth-based tracking of the mars pathfinder lander. J. Geophys. Res. Planets 102, 4057–4064. https://doi.org/10.1029/96JE02125.

Folkner, W.M., Dehant, V., Le Maistre, S., Yseboodt, M., Rivoldini, A., Van Hoolst, T., Asmar, S., Golombek, M., August 2018. The rotation and interior structure experiment on the InSight mission to mars. Space Sci. Rev. 214 (5), 100.

Konopliv, A.S., Yoder, C.F., Standish, E.M., Yuan, D.-N., Sjogren, W.L., May 2006. A global solution for the Mars static and seasonal gravity, Mars orientation, Phobos and Deimos masses, and Mars ephemeris. Icarus 182, 23–50. https://doi.org/10.1016/j.icarus.2005.12.025.

Konopliv, A.S., Park, R.S., Folkner, W.M., August 2016. An improved JPL Mars gravity field and orientation from Mars orbiter and lander tracking data. Icarus 274, 253–260. https://doi.org/10.1016/j.icarus.2016.02.052.

Kouba, J., Mar 2009. Testing of global pressure/temperature (gpt) model and global mapping function (gmf) in gps analyses. J. Geod. 83 (3), 199–208. https://doi.org/10.1007/s00190-008-0229-6, 10.1007/s00190-008-0229-6, ISSN 1432-1394.

Kuchynka, P., Folkner, W.M., Konopliv, A.S., Park, R.S., Le Maistre, S., Dehant, V., February 2014. New constraints on mars rotation determined from radiometric tracking of the opportunity mars exploration rover. Icarus 229, 340–347. https://doi.org/10.1016/j.icarus.2013.11.015. ISSN 0019-1035.

Lagler, K., Schindelegger, M., Bohm, J., Krasna, H., Nilsson, T., 2013. Gpt2: empirical slant delay model for radio space geodetic techniques. Geophys. Res. Lett. 40 (6), 1069–1073. https://doi.org/10.1002/grl.50288. https://agupubs.onlinelibrary.wiley.com/doi/abs/10.1002/grl.50288.

Le Maistre, S., November 2013. The Rotation of Mars and Phobos from Earth-Based Radio-Tracking Observations of a Lander. PhD Thesis. Université Catholique de Louvain.

Le Maistre, S., February 2016. InSight coordinates determination from direct-to-Earth radio-tracking and Mars topography model. Planet. Space Sci. 121 (1–9) https://doi.org/10.1016/j.pss.2015.11.003.

Le Maistre, S., Rosenblatt, P., Rivoldini, A., Dehant, V., Marty, J.-C., Karatekin, Ö., July 2012. Lander radio science experiment with a direct link between Mars and the Earth. Planet. Space Sci. 68 (1), 105–122. https://doi.org/10.1016/j.pss.2011.12.020. ISSN 0032-0633.

Le Maistre, S., Dehant, V., Marty, J.-C., September 2018. Mars nutation estimates from radio-tracking of landed missions prior to InSight and ExoMars 2020. In: European Planetary Science Congress.

Mackenzie, R., Folkner, W.M., October 2006. Applying Appropriate Weights to Doppler Data. Jet Propulsion Laboratory - interoffice memorandum.

Peters, M.-J., Le Maistre, S., Yseboodt, M., Marty, J.-C., Rivoldini, A., Van Hoolst, T., Dehant, V., 2020. LaRa after RISE: Expected Improvement in the Mars Rotation and Interior Models. Planetary and Space Science 180, 104745. https://doi.org/10.1016/j.pss.2019.104745.

Rivoldini, A., Beuthe, M., Van Hoolst, T., Wieczorek, M., Baland, R.-M., Dehant, V., Folkner, W., Gudkova, T., Le Maistre, S., Peters, M.-J., Yseboodt, M., Zharkov, V., 2019. Non-hydrostatic effects on mars' nutation. In: EGU General Assembly Conference Abstracts, ume 21.

Roosbeek, F., 1999. Analytical developments of rigid mars nutation and tide generating potential series. Celest. Mech. Dyn. Astron. 75, 287–300.

Van den Acker, E., Van Hoolst, T., de Viron, O., Defraigne, P., Forget, F., Hourdin, F., Dehant, V., July 2002. Influence of the seasonal winds and the CO_2mass exchange between atmosphere and polar caps on Mars' rotation. J. Geophys. Res. Planets 107, 5055. https://doi.org/10.1029/2000JE001539.

Van Hoolst, T., 2007. The rotation of the terrestrial planets. In: Spohn, T., Schubert, J. (Eds.), Treatise of Geophysics: 'Planets and Moons', ume 10. Elsevier Publ., December, pp. 123–164.

Van Hoolst, T., 2015. 10.04 - rotation of the terrestrial planets. In: Schubert, Gerald (Ed.), Treatise on Geophysics, second ed. Elsevier, Oxford, ISBN 978-0-444-53803-1, pp. 121–151. second ed. edition. http://www.sciencedirect.com/science/article/pii/B9780444538024001688.

Yseboodt, Marie, Dehant, Véronique, Péters, Marie-Julie, 2017. Signatures of the martian rotation parameters in the Doppler and range observables. Planet. Space Sci. 144, 74–88. https://doi.org/10.1016/j.pss.2017.05.008. ISSN 0032-0633.

Zuber, M.T., Lemoine, F.G., Smith, D.E., Konopliv, A.S., Smrekar, S.E., Asmar, S.W., May 2007. Mars reconnaissance orbiter radio science gravity investigation. J. Geophys. Res. Planets 112, E05S07. https://doi.org/10.1029/2006JE002833.